Non-intrusive coupling: recent advances and scalable nonlinear domain decomposition

Mickaël Duval, Jean-Charles Passieux, Michel Salaün, Stéphane Guinard

Noname manuscript No.
(will be inserted by the editor)

Non-intrusive coupling: recent advances and scalable nonlinear domain decomposition

Mickaël Duval · Jean-Charles Passieux · Michel Salaün · Stéphane Guinard

Received: date / Accepted: date

Abstract This paper provides a detailed review of the global/local non-intrusive coupling algorithm. Such method allows to alter a global finite element model, without actually modifying its corresponding numerical operator. We also look into improvement of the initial algorithm (Quasi-Newton and dynamic relaxation), and provide comparison based on several relevant test cases. Innovative examples and advanced applications of the non-intrusive coupling algorithm are provided, granting a handy framework for both researchers and engineers willing to make use of such process. Finally, a novel nonlinear domain decomposition method is derived from the global/local non-intrusive coupling strategy, without the need to use a parallel code or software. Such method being intended to large scale analysis, we show its scalability. Jointly, an efficient high level Message Passing Interface coupling framework is also proposed, granting an universal and flexible way for easy software coupling. A sample code is also given.

Keywords Finite Element Method · Multi-scale · Coupling Algorithms · Non-intrusive · Message Passing Interface · Domain Decomposition

1 Introduction

Simulation in solid mechanics suffers from an intrinsic issue: physical phenomena are complex and heterogeneous, which makes the use of accurate numerical models uneasy. Indeed, simulations are closely bound to computing resources (both hardware and software), which prevents systematic use of complex, accurate numerical models.
Hopefully, most of time simplest models (*i.e.* computationally cheap) are good enough at a

M. Duval · J.C. Passieux · M. Salaün
Université de Toulouse, Institut Clément Ader (ICA),
INSA de Toulouse, UPS, Mines Albi, ISAE,
3 rue Caroline Aigle, 31400 Toulouse, France
E-mail: mickael.duval@univ-tlse3.fr, passieux@insa-toulouse.fr, michel.salaun@isae.fr

S. Guinard
Airbus Group Innovations
BP 90112, 31703 Blagnac, France
E-mail: stephane.guinard@airbus.com

global scale, and one can rely on specific models (*i.e.* complex and computationally expensive) only on small areas, at a local scale.
Such assumption allowed the emergence of a wide variety of numerical methods dedicated to multi-scale and/or multi-model computing. For simplicity of the presentation, we will divide them into two main classes of numerical method: finite element model enrichment and finite element model coupling.

First, one can cite enrichment methods based on the Partition of Unity Method [66]: the Generalised Finite Element Method [81, 27, 53] and the eXtended Finite Element Method [67] being the most famous ones. Their principle is to enrich the finite element functional space with specific functions, which can result from asymptotic expansion [16] or pre-computed local finite element problem solution [18, 19] for instance.
Then, enrichment methods are based on micro-macro models. Their objective is to compute a solution u as a combination of a macro scale solution u^M and a micro scale correction u^m, so that $u = u^M + u^m$. Then the micro scale solution acts as a correction of the macro scale solution, while ensuring unknowns (displacements, forces, stress, strain) equality at the interface between the macro and the micro scale [59, 40]. There exists a wide range of micro-macro methods. The micro model can either be solved analytically as done in the Variational MultiScale method [47], or using the finite element method as well as done by the Strong Coupling Method [48]. When dealing with highly heterogeneous models, the whole macro domain can even be entirely mapped with micro models, as done is the Hierarchical Dirichlet Projection Method [87, 70]. In some cases, micro-macro principle is applied to the finite element solver itself, providing efficient multi-grid numerical methods [78, 73, 36].
Finally, one can also cite structural zooming [25] and finite element patches [76, 77, 55]. The principle of structural zooming is to use a computed global solution as boundary condition for a local refined problem; this method is widespread in structural engineering. Besides, the finite element patches method relies on an iterative process in order to take into account the effect of the local model on the global solution. The main interest of such methods is their ability to compute local corrections in a flexible way, *i.e.* make the local patch definition independent from the global model characteristic.
Following the same idea, structural reanalysis [46, 3] intends to compute *a posteriori* a local correction from a given global solution. In that case, not only the solution is to be corrected, but the global model itself.

Despite all these efforts, it may appear that model enrichment cannot be practically used. Indeed, in an industrial context, most of time one has to rely on existing commercial software which may have been developed and certified for a specific purpose. Though, it is not always easy or even possible to use a given software in order to achieve multi-scale, heterogeneous computation. Moreover, supercomputers recent developments allow to run very ambitious simulations thanks to parallel computations. Thus, instead of embedding all the needing specificities into a unique finite element model, the present-day trend is to rely on model coupling.
Most common coupling methods are based upon iterative sub-structuring algorithms [15, 64], possibly combined with static condensation [35, 85, 86], and Schwarz algorithms [32, 37, 60].
As for the models and/or domains connexions, a wide range of numerical methods are available in the literature. Among them, there is the Mortar method [12, 8, 13] which is based upon weak equality enforcing at the interface through Lagrange multipliers or the Nitsche

method [42, 7, 43, 31, 65, 68]. Besides, energy averaging method, namely the Arlequin method [10, 11, 9] brought a flexible tool for coupling models.

Nevertheless all the above cited methods require quite deep adaptation or modification of finite element solvers and software, which is not always doable in an industrial context.
More recently, a new class of method is emerging: the non-intrusive coupling. It allows to locally modify an existing finite element model, without actually altering its corresponding numerical operator [82, 34].
Thus, a main consequence of non-intrusiveness is the possibility to easily merge commercial software and research codes, as no modification of the software will be required. In addition, such algorithm will easily fit the standard input/output specifications of most industrial software.
Actually, the non-intrusive global/local coupling strategy is currently under investigation through several applications.
One can cite crack propagation [74, 41]. In that case, a two-level non-intrusive coupling is proposed, either within a multi-grid or a GFEM framework: a first global model is used in order to represent the global structure behaviour, a second local model takes into account the crack.
Then, non-intrusive coupling is also investigated within a stochastic framework [21]. The objective is here to take into account local uncertainties into a global problem with deterministic operator, using a non-intrusive strategy. The main property of such coupling is its ability to represent the stochastic effect of the local uncertainties at the global scale without altering the initial global deterministic operator.
One can finally cite 2D/3D coupling [39]. The strategy developed here aims at coupling a global plate model with local 3D models on localised zones where plate modelling is inadequate.
All in all, such flexible method can be applied to a very wide variety of static mechanical analysis, including quasi-static crack propagation, plasticity, contact, composite failure [24],... , and even transient dynamics problems [14, 20].

In this paper, we propose to analyse the effectiveness of this algorithm through various applications (crack, plasticity, contact), and a comparative analysis of some existing acceleration methods in the literature.
It is also proposed to extend the method to the case of multiple patches. We also show that this type of method can be used to locally redefine the geometry and boundary conditions.

In fact, model coupling is also widely used for domain decomposition. Among them one can cite the well-known Finite Element Tearing and Interconnecting method [28], the Balanced Domain Decomposition method [62] and the LArge Time INcremental method [58] which are the most used in structural engineering.
In that context, nonlinear localisation algorithms have also recently been proposed [23, 75, 6, 5]. The objective of nonlinear localisation algorithm is to bring an efficient way to apply domain decomposition method to nonlinear problem through the general Newton-Krylov-Schur solvers class.

We then propose a new algorithm for nonlinear domain decomposition based on the concept of non-intrusive coupling.
All the examples illustrated in this paper have been computed using *Code_Aster*, an open source software package for numerical simulation in structural mechanics developed by the

French company EDF [88] for industrial applications. The complete code used to run one of the given examples is also provided as appendix.

2 Non-intrusive coupling: a state of the art

2.1 Mechanical problem

Let us consider an elastic body represented by a geometrical domain Ω. Displacement u_D is prescribed on the Dirichlet boundary Γ_D, surface force f_N is applied on the Neumann boundary Γ_N and body force f_Ω is applied on Ω. Then we seek to solve the following mechanical problem:

$$(\mathscr{P}): \quad \min_{u\in\mathscr{U}} \quad J(u) \tag{1}$$

For the sake of simplicity, we consider here a linear elastic model ($\mathbf{C}$ being the corresponding Hooke tensor and ε being the infinitesimal strain tensor). We then give the definition of the affine space $\mathscr{U}$ (we will also make use of its corresponding vector space $\mathscr{U}^0$) and the potential function J.

$$\mathscr{U} = \{u \in H^1(\Omega),\ u|_{\Gamma_D} = u_D\} \tag{2}$$

$$\mathscr{U}^0 = \{u \in H^1(\Omega),\ u|_{\Gamma_D} = 0\} \tag{3}$$

$$J(u) = \frac{1}{2}\int_\Omega \mathbf{C}\varepsilon(u(x)) : \varepsilon(u(x))dx - \int_{\Gamma_N} f_N(x)\cdot u(x)dx - \int_\Omega f_\Omega(x)\cdot u(x)dx \tag{4}$$

In the context of the finite element method, we will make use of the equivalent variational formulation

$$u \in \mathscr{U},\ \ \forall v \in \mathscr{U}^0,\ \ a(u,v) = l(v) \tag{5}$$

with the following definition of the bilinear and linear forms a and l:

$$a(u,v) = \int_\Omega \mathbf{C}\varepsilon(u(x)) : \varepsilon(v(x))dx \tag{6}$$

$$l(v) = \int_{\Gamma_N} f_N(x)\cdot v(x)dx + \int_\Omega f_\Omega(x)\cdot v(x)dx \tag{7}$$

When using the finite element method to solve such a problem, a mesh will be set up, a stiffness matrix and a right hand side vector will be assembled, and finally a linear system will be solved. Now, let us consider that a local detail is missing from the modelling (crack, hole,...). One cannot easily use the initial homogeneous model defined above, as it would require to adapt it. When the detail location is not known *a priori*, such model adaptation can be very intrusive and computationally expensive.
Then a possible way to deal with heterogeneous models is to use domain decomposition based model coupling, each domain being represented with its own *ad hoc* model. Without loss of generality, we will take here the example of a cracked domain (see Fig. 1). The domain is then divided into a global part Ω_G and a local part Ω_L, thus those two non-overlapping sub-domains share a common interface Γ. The Dirichlet and Neumann boundaries are also partitioned as following:

- $\Gamma_{D,G} = \Gamma_D \cap \partial\Omega_G$ and $\Gamma_{D,L} = \Gamma_D \cap \partial\Omega_L$
- $\Gamma_{N,G} = \Gamma_N \cap \partial\Omega_G$ and $\Gamma_{N,L} = \Gamma_N \cap \partial\Omega_L$

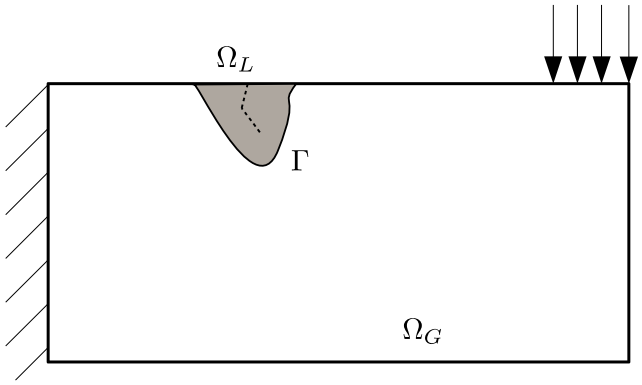

Fig. 1: Situation overview: global/local mechanical problem

We then need to define new functional spaces in order to give an adapted formulation to the global/local problem, $\mathscr{U}_G$ and $\mathscr{U}_L$ (and their corresponding vector spaces $\mathscr{U}_G^0$ and $\mathscr{U}_L^0$).

$$\mathscr{U}_G = \{u \in H^1(\Omega_G),\ \ u|_{\Gamma_{D,G}} = u_D\} \tag{8}$$

$$\mathscr{U}_L = \{u \in H^1(\Omega_L),\ \ u|_{\Gamma_{D,L}} = u_D\} \tag{9}$$

We also consider $\mathscr{U}_\psi \subset L^2(\Gamma)$ the Lagrange multipliers functional space.
Displacement and efforts continuity will be imposed in a weak sense *via* a mortar method at the interface [12, 8, 13, 33]. We then get the following dual formulation for the domain decomposition problem:

$$\begin{aligned} &u_G \in \mathscr{U}_G,\ \ u_L \in \mathscr{U}_L,\ \ \psi \in \mathscr{U}_\psi \\ &\forall v_G \in \mathscr{U}_G^0,\ \ a_G(u_G, v_G) + b(\psi, v_G) = l_G(v_G) \\ &\forall v_L \in \mathscr{U}_L^0,\ \ a_L(u_L, v_L) - b(\psi, v_L) = l_L(v_L) \\ &\forall \vartheta \in \mathscr{U}_\psi,\ \ b(\vartheta, u_G - u_L) = 0 \end{aligned} \tag{10}$$

where the definitions of the bilinear forms a_G, a_L and b are given below.

$$a_G(u,v) = \int_{\Omega_G} \mathbf{C}\varepsilon(u(x)) : \varepsilon(v(x))dx \tag{11}$$

$$a_L(u,v) = \int_{\Omega_L} \mathbf{C}\varepsilon(u(x)) : \varepsilon(v(x))dx \tag{12}$$

$$l_G(v) = \int_{\Gamma_{N,G}} f_N(x) \cdot v(x)dx + \int_{\Omega_G} f_\Omega(x) \cdot v(x)dx \tag{13}$$

$$l_L(v) = \int_{\Gamma_{N,L}} f_N(x) \cdot v(x)dx + \int_{\Omega_L} f_\Omega(x) \cdot v(x)dx \tag{14}$$

$$b(\vartheta, u) = \int_\Gamma \vartheta(x) \cdot u(x)dx \tag{15}$$

According to our example (the locally cracked body), one can use a standard Finite Element Method (FEM) on the global part, and an eXtended Finite Element Method (XFEM, [67]) on the local cracked part (another solution would be to rely on an analytical model for the local part , [80]), as it is done in [86, 85]. Let us define φ_G, φ_L and φ_ψ the basis functions

of the finite element spaces corresponding to the discretization of $\mathscr{U}_G$, $\mathscr{U}_L$ and $\mathscr{U}_\psi$. We will give more details on the discretization of the Lagrangian dual space further, still it may be noted that the mortar coupling used here allows non-conforming meshes at the interface Γ.
Let us also consider the triangulations $\mathscr{T}_G$ and $\mathscr{T}_L$ of Ω_G and Ω_L respectively, and $\mathscr{T}_{\Gamma,G}$ and $\mathscr{T}_{\Gamma,L}$ their restriction on Γ. We will denote n_G the number of degrees of freedom of $\mathscr{T}_G$ and $n_{\Gamma,G}$ the number of degrees of freedom of $\mathscr{T}_{\Gamma,G}$. Then n_L and $n_{\Gamma,L}$ will follow the same definition on the local domain. Finally, $\mathscr{T}_{\Gamma,\psi}$ will stands for the Lagrangian multipliers mesh on the interface Γ, with $n_{\Gamma,\psi}$ its number of degrees of freedom.
Then we can define the finite element matrices (stiffness matrices, coupling matrices and right-hand side vector):

– the stiffness matrices K_G ($n_G \times n_G$ matrix) and K_L ($n_L \times n_L$ matrix)

$$(K_G)_{ij} = \int_{\Omega_G} \mathbf{C}\varepsilon(\varphi_G^i(x)) : \varepsilon(\varphi_G^j(x))dx \tag{16}$$

$$(K_L)_{ij} = \int_{\Omega_L} \mathbf{C}\varepsilon(\varphi_L^i(x)) : \varepsilon(\varphi_L^j(x))dx \tag{17}$$

– the right-hand side load vectors F_G (vector of size n_G) and F_L (vector of size n_L)

$$(F_G)_j = \int_{\Gamma_{N,G}} f_N(x) \cdot \varphi_G^j(x)dx + \int_{\Omega_G} f_\Omega(x) \cdot \varphi_G^j(x)dx \tag{18}$$

$$(F_L)_j = \int_{\Gamma_{N,L}} f_N(x) \cdot \varphi_L^j(x)dx + \int_{\Omega_L} f_\Omega(x) \cdot \varphi_L^j(x)dx \tag{19}$$

– the coupling matrices C_G ($n_{\Gamma,\psi} \times n_{\Gamma,G}$ matrix) and C_L ($n_{\Gamma,\psi} \times n_{\Gamma,L}$ matrix)

$$(C_G)_{ij} = \int_\Gamma \varphi_\psi^i \cdot \varphi_G^j dx \tag{20}$$

$$(C_L)_{ij} = \int_\Gamma \varphi_\psi^i \cdot \varphi_L^j dx \tag{21}$$

If one had to use a monolithic solver when computing the solution of Eq. (10), the resulting finite element linear system would be the following:

$$\begin{bmatrix} K_G & 0 & \underline{C_G}^\top \\ 0 & K_L & -\underline{C_L}^\top \\ \underline{C_G} & -\underline{C_L} & 0 \end{bmatrix} \begin{bmatrix} U_G \\ U_L \\ \Psi \end{bmatrix} = \begin{bmatrix} F_G \\ F_L \\ 0 \end{bmatrix} \tag{22}$$

Remark: In order to simplify notations, we decided to not explicitly use restriction and prolongation operators. Instead, we will denote the restriction operation with $\cdot|$, and the prolongation operation with $\underline{\cdot}$ each time it is needed. Such restriction and prolongation operators are merely boolean-matrix based operators which cast a shape-given object into an other one by gathering selected values or by supplementing it with zeros.
For instance, we define here $\underline{C_G}$ the prolongation of C_G from $\mathscr{T}_{\Gamma,\psi} \times \mathscr{T}_{\Gamma,G}$ to $\mathscr{T}_{\Gamma,\psi} \times \mathscr{T}_G$. Then $\underline{C_G}$ stands for a matrix of shape $n_{\Gamma,\psi} \times n_G$, all the remaining coefficients being filled with zeros. The same procedure defines $\underline{C_L}$, the prolongation of C_L from $\mathscr{T}_{\Gamma,\psi} \times \mathscr{T}_{\Gamma,L}$ to $\mathscr{T}_{\Gamma,\psi} \times \mathscr{T}_L$.

Remark: It is not an easy task to set up a "good" basis of $\mathscr{U}_\psi$ when discretizing the Lagrange multipliers [83, 84]. If the basis is bad-chosen (*i.e.* the *inf-sup* conditions are not

fulfilled), the mortar operator can lead to undesirable energy-free oscillations of the displacement fields. For the sake of ease, we chose in this paper to use the local finite element basis on the interface for the Lagrange multiplier as well (*i.e.* $\mathscr{T}_{\Gamma,\psi} = \mathscr{T}_{\Gamma,L}$ and $\varphi_\psi = \varphi_L$ on Γ). The main consequence of such a choice is that matrix C_L is a square invertible matrix: we will not have to rely on least squares methods (*i.e.* generalised inverse matrix) when performing the interface projections. We never encountered instabilities in all the test cases we set up using that Lagrange multipliers basis.

Of course, the idea behind such a domain decomposition is to dissociate Ω_G and Ω_L when solving the problem. A solution is to set up an asymmetric global/local algorithm, *i.e.* solving alternately Dirichlet and Neumann problems on the local and global models until convergence.
To that end, let us define interface projection like operator P and $P^\top$ from the global to the local model and from the local to the global model respectively, so that $P = C_L^{-1} C_G$ and $P^\top = C_G^\top C_L^{-\top}$).

We will also denote $\Lambda_G = (K_G U_G - F_G)|_\Gamma$ and $\Lambda_L = (K_L U_L - F_L)|_\Gamma$ the global and local reaction forces at the interface Γ.

Algorithm 1: Global/local domain decomposition – Fixed point solver

Data: ε, Λ_L^0
k = 0
while $\eta > \varepsilon$ **do**
Global problem computation (Neumann problem)
$K_G U_G^{k+1} = F_G - \underline{P}^\top \underline{\Lambda}_L^k$
Local problem computation (Dirichlet problem)
$$\begin{bmatrix} K_L & -\underline{C_L}^\top \\ -\underline{C_L} & 0 \end{bmatrix} \begin{bmatrix} U_L^{k+1} \\ \Psi^{k+1} \end{bmatrix} = \begin{bmatrix} F_L \\ -C_L P\, U_G^{k+1}|_\Gamma \end{bmatrix}$$
Convergence test
$\eta = \|\Lambda_G^{k+1} + P^\top \Lambda_L^{k+1}\| / \sqrt{\|F_G\|^2 + \|F_L\|^2}$
k = k+1
end
Result: U_G^k, U_L^k

The convergence test used here relies on the reaction equilibrium between the two domains.

Global/local model coupling is a powerful tool to handle heterogeneity at a local scale when performing structural analysis. Nevertheless, it implies to set up the two models each time one wants to run a computation. For instance, in our example, if the crack grows, the mesh partitioning will not stand right for long; then one needs to adapt both global and local models, which can be very time consuming (in terms of human and computer resources). Still, there exists a way to keep a global model unchanged when performing a global/local computation: the non-intrusive coupling [82].

2.2 Global/local non-intrusive coupling method

The principle of non-intrusive coupling is to rely on an existing global model on $\Omega = \Omega_G \cup \Omega_{\widetilde{G}}$ (see Fig. 2), its triangulation $\mathscr{T}$, and its corresponding stiffness matrix K (a $n \times n$ matrix).
From now on, we denote $\mathscr{T}_{\widetilde{G}}$ the triangulation of $\Omega_{\widetilde{G}}$ and the corresponding stiffness ma-

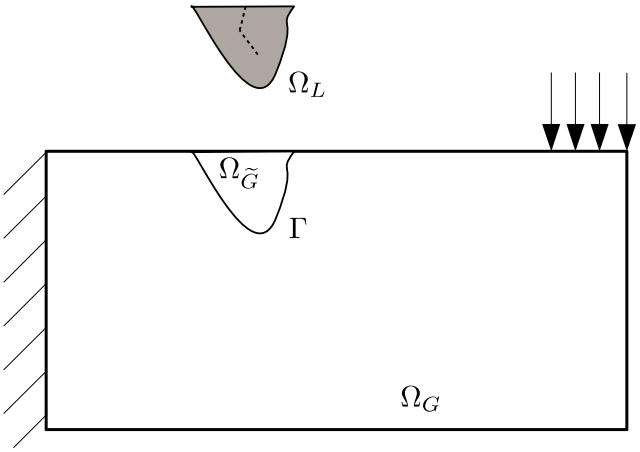

Fig. 2: Situation overview: non-intrusive global/local problem

trix $K_{\widetilde{G}}$ (a $n_{\widetilde{G}} \times n_{\widetilde{G}}$ matrix). As $\mathscr{T}_{\widetilde{G}}$ is a part of $\mathscr{T}$ (*i.e.* $\mathscr{T} = \mathscr{T}_G \cup \mathscr{T}_{\widetilde{G}}$), we naturally have $\mathscr{T}_{\Gamma,G} = \mathscr{T}_{\Gamma,\widetilde{G}}$.
Then the objective is to replace the global model on $\Omega_{\widetilde{G}}$ by the local one on Ω_L without actually modifying the global finite element operator K on Ω. From a practical point of view, we define U the fictitious prolongation of U_G to the full domain Ω, so that $U|_{\Omega_G} = U_G$ and $U|_{\Omega_{\widetilde{G}}} = U_{\widetilde{G}}$ (*i.e.* $U_{\widetilde{G}}$ is the prolonged part of the global solution U).
In our example, such a prolonged model will stand to a standard FEM model, the crack being absent from the prolongation.
We define $F = \underline{F}_G + \underline{F}_{\widetilde{G}}$ the load vector defined on Ω. Then, applying the Chasles relation on Eq. (11) in the discrete form gives us the following equality which will be used to adapt Alg. 1.

$$KU = \underline{K}_G U + \underline{K}_{\widetilde{G}} U \tag{23}$$

Using this equality at the global computation step gives us the expression of the equation standing for the global model at each iteration k, with $\Lambda_{\widetilde{G}} = (K_{\widetilde{G}} U_{\widetilde{G}} - F_{\widetilde{G}})\big|_\Gamma$.

$$KU^{k+1} = F - \underline{P}^\top \underline{\Lambda}_L^k + \underline{\Lambda}_{\widetilde{G}}^k \tag{24}$$

The global/local coupling algorithm can then be given in its non-intrusive form.

Algorithm 2: Global/local domain decomposition – Non-intrusive fixed point solver

Data: ε, Λ_L^0, $\Lambda_{\widetilde{G}}^0$
k = 0
while $\eta > \varepsilon$ **do**
Global problem computation
$$KU^{k+1} = F - \underline{P}^{\top}\,\underline{\Lambda}_L^k + \underline{\Lambda}_{\widetilde{G}}^k$$
Local problem computation
$$\begin{bmatrix} K_L & -\underline{C}_L^{\top} \\ -\underline{C}_L & 0 \end{bmatrix} \begin{bmatrix} U_L^{k+1} \\ \Psi^{k+1} \end{bmatrix} = \begin{bmatrix} F_L \\ -C_L P\, U^{k+1}\big|_{\Gamma} \end{bmatrix}$$
Convergence test
$$\eta = \|\Lambda_G^{k+1} + P^{\top}\Lambda_L^{k+1}\| / \sqrt{\|F_G\|^2 + \|F_L\|^2}$$
k = k+1
end
Result: U^k, U_L^k

It must be noted that, thanks to the prolongation of the global model (*i.e.* the non-intrusiveness of the coupling), the stiffness matrix K will be assembled and factorised only once. In our example, even if the crack grows, the global model will stand unmodified. The coupling will only involve displacements and forces exchange at the interface Γ (see Fig. 3). It may

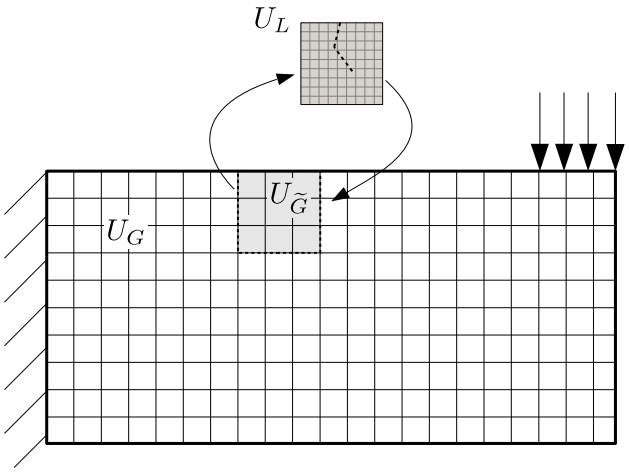

Fig. 3: Situation overview: non-intrusive coupling

also be noted that the fictitious prolongation of the global solution U on $\Omega_{\widetilde{G}}$ has no physical meaning, and that its value depends on the initialisation (*i.e.* the values of Λ_L^0 and $\Lambda_{\widetilde{G}}^0$). Nevertheless, as such fictitious solution has to be replaced by the one obtained from the local model, that is of no consequence.
There are several advantages arising from non-intrusive coupling:

- the global mesh on Ω is always left unchanged (so is the global stiffness matrix K), which is convenient when the objective is to investigate local details on large scale structures (*i.e.* involving a large number of degrees of freedom)

- when dealing with local nonlinear details (we will present applications involving nonlinear local behaviour further), one can use a linear (*i.e.* fast) solver for the global model and use a nonlinear solver only for the local part
- the local model acts as a correction applied to the global model on the right-hand side, so that different research codes or commercial software can be easily merged in a non-intrusive way.

2.3 Incremental formulation – Additive global correction

The main drawback of Alg. 2 is its low convergence speed. In fact, the convergence speed depends of the stiffness gap between Ω_L and $\Omega_{\widetilde{G}}$: the more the gap is important, the more the convergence is slow. Such phenomenon is not shown to be significant for local plasticity problem [34, 61]. In our example, we shall see that it can be a severe disadvantage when the crack grows: the stiffness gap increases as the crack spreads since the global model does not include any representation of the crack. Then, acceleration techniques will be used in order to improve the convergence speed of the algorithm.
We propose in that section an incremental formulation of the non-intrusive global/local algorithm as a prerequisite for the acceleration technique setting up.

First of all, let us remark the following equilibrium equation of the global model at iteration k:

$$KU^k = F + \underline{\Lambda}_G^k + \underline{\Lambda}_{\widetilde{G}}^k \tag{25}$$

It is possible to reformulate Alg. 2 into a Newton-like algorithm (*i.e.* in an incremental formulation) by adding a $-KU^k$ term both on the left and right side of the global domain equation at iteration k.

$$K\left(U^{k+1} - U^k\right) = F - \underline{P}^\top \underline{\Lambda}_L^k + \underline{\Lambda}_{\widetilde{G}}^k - KU^k \tag{26}$$

Indeed, making use of Eq. (25) into Eq. (26), one can give the following formulation:

$$U^{k+1} = U^k - K^{-1} f(U^k) \tag{27}$$

where f is the finite element operator computing the forces equilibrium residual between Ω_G and Ω_L given the global displacement U^k at iteration k.

$$f(U^k) = \underline{\Lambda}_G^k + \underline{P}^\top \underline{\Lambda}_L^k \tag{28}$$

One can remark that Eq. (27) looks very much like a modified Newton method prescribed on $f = 0$ (we look for the solution which verify the interface forces equilibrium). In fact, let us show now that $K \approx \nabla f$.
Let us define S_L and $S_{\widetilde{G}}$ the primal Schur complements (Dirichlet problem with prescribed displacement on Γ) corresponding to the local model K_L and to the fictitious global model $K_{\widetilde{G}}$ respectively [38]. Then we get the following condensed equilibrium equations on the interface Γ:

$$\Lambda_L = S_L P\, U|_\Gamma \tag{29}$$
$$\Lambda_{\widetilde{G}} = S_{\widetilde{G}}\, U|_\Gamma \tag{30}$$

We then introduce $\Lambda_{\widetilde{G}}$ in Eq. (28) so that it can be rewritten in the following way:

$$f(U^k) = \underline{\Lambda}_G^k + \underline{P}^\top \underline{\Lambda}_L^k + \underline{\Lambda}_{\widetilde{G}}^k - \underline{\Lambda}_{\widetilde{G}}^k \tag{31}$$

Still, from Eq. (25) we have $\underline{\Lambda}_G^k + \underline{\Lambda}_{\widetilde{G}}^k = KU^k - F$. We finally get the exact formulation of the interface residual function f.

$$f(U^k) = KU^k - F + (\underline{P}^\top \underline{S}_L \underline{P} - \underline{S}_{\widetilde{G}})U^k \tag{32}$$

We can then give the expression for ∇f:

$$\nabla f = K + (\underline{P}^\top \underline{S}_L \underline{P} - \underline{S}_{\widetilde{G}}) \tag{33}$$

It can be seen that K is a good approximation of ∇f as soon as the condensed stiffness between the local and the global models at the interface are close.

$$\|\nabla f - K\| = \|\underline{P}^\top \underline{S}_L \underline{P} - \underline{S}_{\widetilde{G}}\| \tag{34}$$

In practice (*e.g.* local cracked domain, see Fig. 3), the previous hypothesis does not stand for true any longer: in that case, matrix K is a bad approximation of the true gradient ∇f. Thus, the modified Newton scheme (27), when used as such, would lead to tremendous iterations number when the crack grows.
In fact, as soon as Ω_L is stiffer than $\Omega_{\widetilde{G}}$, the algorithm becomes divergent [21].

2.4 Convergence properties – Relaxation

In our case Eq. (27) is fully equivalent to the fixed point equation prescribed on $g(U) = U$ with the following definition of g.

$$g(U) = U - K^{-1} f(U) \tag{35}$$

Then, using relaxation (with a well-chosen constant parameter ω) enforces stability of the numerical scheme, ensuring convergence of the algorithm even if Ω_L is stiffer than $\Omega_{\widetilde{G}}$. In the present situation, relaxation will consist in a two-step computation at iteration k. First a predicted value $\bar{U}^{k+1}$ is computed from the previous solution U^k, then this value is corrected using a relaxation parameter ω.

$$\bar{U}^{k+1} = g(U^k) \tag{36}$$
$$U^{k+1} = \omega \bar{U}^{k+1} + (1-\omega)U^k \tag{37}$$

The optimal relaxation parameter ω can be computed upon the knowledge of the eigenvalues of the iteration operator [21], or using a power-type method during the first global/local iterations in order to get an cheaper approximation.
Still, computing a good relaxation parameter remains computationally very expensive.

2.5 Dynamic relaxation: Aitken's Delta Squared acceleration

Then a possibility is to rely on dynamic relaxation, *i.e.* computing a new parameter ω_k for each iteration, assuming that we can provide an easy and cheap way for the computation of ω_k.

$$\bar{U}^{k+1} = g(U^k) \tag{38}$$
$$U^{k+1} = \omega_k \bar{U}^{k+1} + (1-\omega_k)U^k \tag{39}$$

In this paper, we investigate dynamic relaxtion based upon the Aitken's Delta Squared formula [49, 54, 61], also used in Fluid-Structure Interaction (FSI).
Let us define the predicted displacement increment δ such as $\delta_{k+1} = (\bar{U}^{k+1} - U^k)|_\Gamma$. Then the relaxation parameter ω is dynamically updated following the recursive formula below.

$$\omega_{k+1} = -\omega_k \frac{\delta_{k+1}^\top (\delta_{k+2} - \delta_{k+1})}{\|\delta_{k+2} - \delta_{k+1}\|^2} \tag{40}$$

No relaxation is applied to the first two iterations ($U^0 = \bar{U}^0$ and $U^1 = \bar{U}^1$) and the relaxation parameter initial value is set to $\omega_0 = 1$.
The Aitken's Delta Squared method involves very few computing overhead, as it only involve displacement value at the interface obtained from the two previous iterations. Moreover, such method will be shown to improve the convergence speed of the initial algorithm.

2.6 Quasi-Newton acceleration

An other possible way to speed up the convergence is to rely on Quasi-Newton methods to update matrix K. The Symmetric Rank One (SR1) update is an easy-to-implement and efficient way to build a sequence of matrices K_k convergent toward ∇f, assuming $K_0 = K$ when initialising the algorithm [22, 51, 50, 69, 34, 52].
Let us define $d_k = U^{k+1} - U^k$ and $y_k = f(U^{k+1}) - f(U^k)$. At iteration k, we seek to update K_k into K_{k+1} with the SR1 formula, *i.e.* with a rank-one symmetric update, while verifying the secant equation for each iteration $k > 1$:

$$K_{k+1} = K_k + \rho v v^\top \tag{41}$$
$$K_{k+1} d_k = y_k \tag{42}$$

In Eq. (41), v is a vector with the same shape than U and $\rho = \pm 1$. Then, making use of Eq. (41) into Eq. (42) gives us the following relation:

$$y_k - K_k d_k = \rho v v^\top d_k \tag{43}$$

As it can be seen in Eq. (43), $y_k - K_k d_k$ and v are collinear ($\rho v^\top d_k$ being a scalar), thus there exists a real α such as v get the following expression:

$$v = \alpha(y_k - K_k d_k) \tag{44}$$

Then, again from Eq. (43), we have $d_k^\top (y_k - K_k d_k) = \rho d_k^\top v v^\top d_k$ which leaves us with

$$\rho = \mathrm{sgn}\{d_k^\top (y_k - K_k d_k)\} \tag{45}$$

as $vv^\top$ is a positive-semidefinite matrix. Finally, the value of α arises using Eq. (44) into Eq. (43).

$$\alpha^2 = \frac{1}{\left| d_k^\top (y_k - K_k d_k) \right|} \tag{46}$$

All in all, one can retrieve the well-known SR1 update formula:

$$K_{k+1} = K_k + \frac{(y_k - K_k d_k)(y_k - K_k d_k)^\top}{d_k^\top (y_k - K_k d_k)} \tag{47}$$

Note that in the context of the SR1 update, Eq.(27) rewrites $K_k d_k = -f_k$, so that Eq. (47) can be given in a simplified form (where $f_k = f(U^k)$):

$$K_{k+1} = K_k + \frac{f_{k+1} f_{k+1}^\top}{d_k^\top f_{k+1}} \tag{48}$$

Finally, thanks to the SR1 formula, we get a simple expression of the tangent matrix update for each iteration k. Nevertheless, one has to keep in mind the non-intrusiveness constraint of the coupling algorithm, *i.e.* do not modify the global stiffness matrix K. This can be achieved using the Sherman-Morrison formula on Eq. (48), leaving us with the following relation which can be used in order to compute $K_k^{-1} f$ in a iterative manner based upon the knowledge of $K_0^{-1} f$.

$$K_{k+1}^{-1} = K_k^{-1} - K_k^{-1} f_{k+1} \frac{f_{k+1}^\top K_k^{-1}}{f_{k+1}^\top (d_k + K_k^{-1} f_{k+1})} \tag{49}$$

We give here the algorithmic version of such iterative relation [34].

Algorithm 3: Non-intrusive global correction

Data: f_k
$i = 0$
Compute $K_0^{-1} f_k$
while $i < k$ **do**
  $K_{i+1}^{-1} f_k = K_i^{-1} f_k - K_i^{-1} f_{i+1} \frac{f_{i+1}^\top K_i^{-1} f_k}{f_{i+1}^\top (d_i + K_i^{-1} f_{i+1})}$
  $i = i + 1$
end
$d_k = -K_k^{-1} f_k$
Result: d_k

At iteration k, we suppose that $\{(f_i)_{i<k}\}$, $\{(d_i)_{i<k}\}$,$\{(K_i^{-1} f_{i+1})_{i<k-1}\}$ have been stored from the previous iterations. The overhead involved by the non-intrusive SR1 formula remains very low compared to the acceleration provided in terms of convergence speed. Indeed, it can be seen in Alg. 3 that, at iteration k, the global solver is called only once when computing $K_0^{-1} f_k$; then the value of $K_k^{-1} f_k$ is computed recursively and requires only scalar products on the interface Γ.

2.7 Non-intrusive coupling illustration: crack growth simulation

Actually, crack propagation is the most obvious example of local detail whose effects on the global structure are the most visible (structure failure in the worst case).
In this section, we give a simple example to illustrate the non-intrusive global/local coupling algorithm and its properties.
We consider here a rectangular two-dimensional domain (200×80 *mm*). The material law is linear elastic in plane strain conditions ($E = 200$ *GPa* and $\nu = 0.3$) and the global loading is represented by a uniform pressure of magnitude 10 *MPa* as depicted in Fig. 2. The initial crack is defined by a vertical notch extending from the crack tip position ($x_{ct} = -50$ *mm* and $y_{ct} = 35$ *mm* from the center of the plate).
We investigated quasi-static crack growth simulation using the non-intrusive coupling method presented in the previous sections. We computed fourteen quasi-static propagation steps, using a constant growth increment $\Delta = 3.75$ *mm* (this value is linked to the patch mesh size at crack tip, h_{ct}, such as $\Delta = 8h_{ct}$). For each step, the crack bifurcation angle is determined using the maximal hoop stress criterion.
We give in Fig. 4 an illustration of the displacement field (modulus) from the last prop-

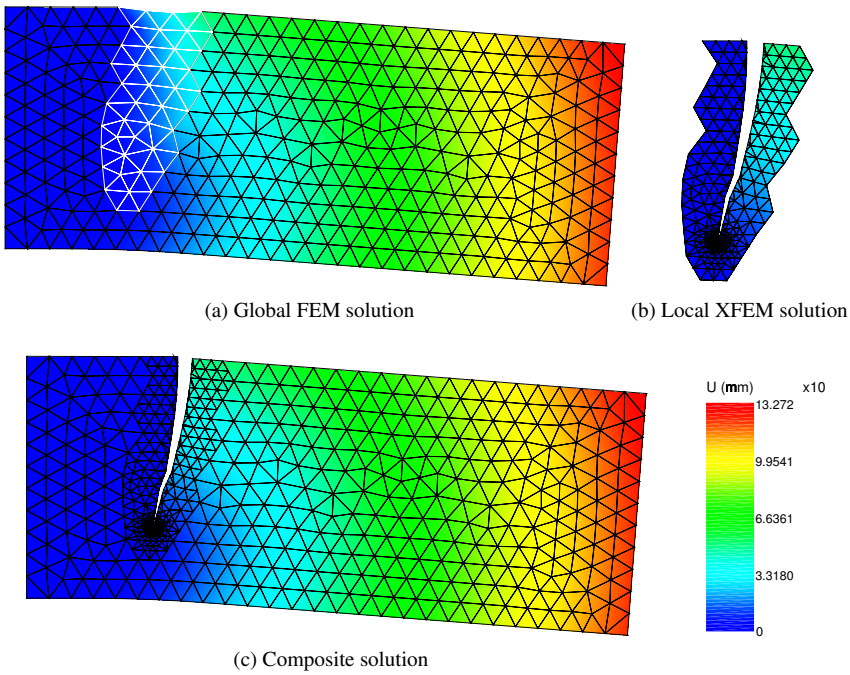

(a) Global FEM solution (b) Local XFEM solution

(c) Composite solution

Fig. 4: Non-intrusive crack growth simulation

agation step. As one may notice, the initial mesh on Ω (see Fig. 4a) is unaffected by the crack spreading, while the global solution is. Global and local meshes are not bound to be coinciding at the interface, allowing for a flexible local mesh refinement.
We applied both Quasi-Newton SR1 and Aitken's Delta Squared acceleration techniques to the non-intrusive coupling algorithm with relative tolerance $\varepsilon = 10^{-10}$ for each crack prop-

agation step.
The main properties of the coupling algorithm and the acceleration techniques can be pulled out from Fig. 5. The first graph gives the link between the crack length and the number of iterations needed to reach the equilibrium, and the second one represents the residual evolution over the algorithm iterations (for the last crack propagation step).
Two main observations can be underlined. First, it can be observed in Fig. 5a that, using no acceleration, the number of iterations required to reach the chosen tolerance ε is strongly dependant of the crack length (*i.e.* the stiffness gap between the local XFEM model and the global FEM model, as shown in Eq. (34)). The Quasi-Newton acceleration allows to nearly get rid of such problem as the tangent stiffness of the FEM model is updated through the SR1 procedure, in a non-intrusive way.
When focusing on a specific crack propagation step (here the final one, see Fig. 5b), the different acceleration techniques show quite heterogeneous results. First, the number of iterations required to reach the given precision when no acceleration is used is clearly not affordable compared to the other results. In the context of crack propagation, the Aitken's Delta Squared method proves to be less efficient than the Quasi-Newton acceleration. In the present case, the last propagation step took 3006 iterations without any acceleration to converge, 389 with the Aitken's accelerator and 18 using the Quasi-Newton update.
Note that as soon as the crack nearly divides the plate into two parts, one can no longer reasonably speak of "global/local" situation. Nevertheless, nothing prevents the coupling scheme to be applied to such critical situation, which allows us to distinctly analyse the differences between the two acceleration techniques.

2.8 Patch geometry: influence on the convergence speed

In the previous example, the patch is defined on the region of interest which needs to get worked out with a specific local model (the crack). However, we never gave details about how is defined the patch, and what is the influence of its spatial extend until now.
In fact, there is no constrain nor generic rule about the way to define the patch extend. In the crack propagation case, we simply select a given number of stitch layers from the global mesh around the crack location. Then those stitches are duplicated and saved as local mesh (see Fig. 4a and 4b). Any refinement of the freshly generated local mesh is possible, particularly at crack tip.
Nevertheless, the patch extend is not without consequence on the algorithm convergence properties. Indeed, as said previously, the convergence rate depends on the stiffness gap between the local and the global model. Let us consider the bending plate case with a static crack defined by a vertical ray extending from the crack tip position ($x_{ct} = 0$ *mm* and $y_{ct} = 10$ *mm* from the center of the plate). We applied the non-intrusive coupling algorithm considering several patch thicknesses (one to ten global stitches layers), as depicted on Fig. 6. In the present example, the global model stands for a non-cracked plate whereas the local model stands for the cracked one. According to the Saint-Venant principle, the crack influence will decrease when getting far from the perturbation. Thus, the more the patch extends far from the crack, the less the stiffness gap between the global and the local model will be important, allowing for faster convergence (this is numerically illustrated on Fig 7). Moreover such phenomenon can be observed both with standard and accelerated algorithms. Nevertheless the Quasi-Newton update is the only one guaranteeing a reasonable number of iterations which is almost independent from the patch thickness.

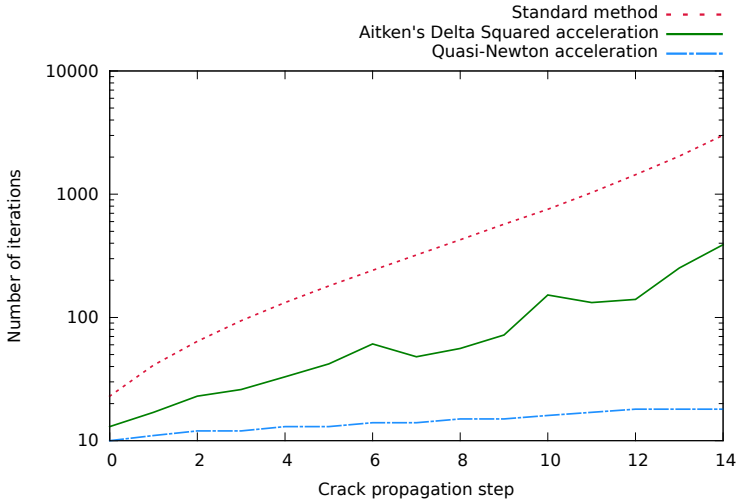

(a) Crack spreading: dependence between crack length and convergence speed

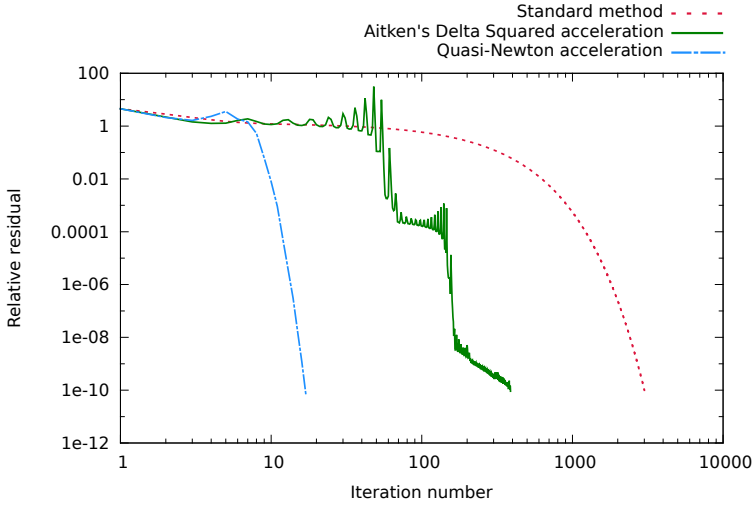

(b) Final crack propagation step: residual evolution

Fig. 5: Crack growth simulation: acceleration techniques comparison

Still one should keep in mind that the more the patch extends, the more it will be computationally expensive to work out as it will involve a larger number of degrees of freedom, particularly in the nonlinear case. Meanwhile, the local patch should be large enough in order to fully take into account the local behaviour (XFEM enrichment for instance). Then engineer's skills must prevail in order to determine the best choice of parameters in such situations.

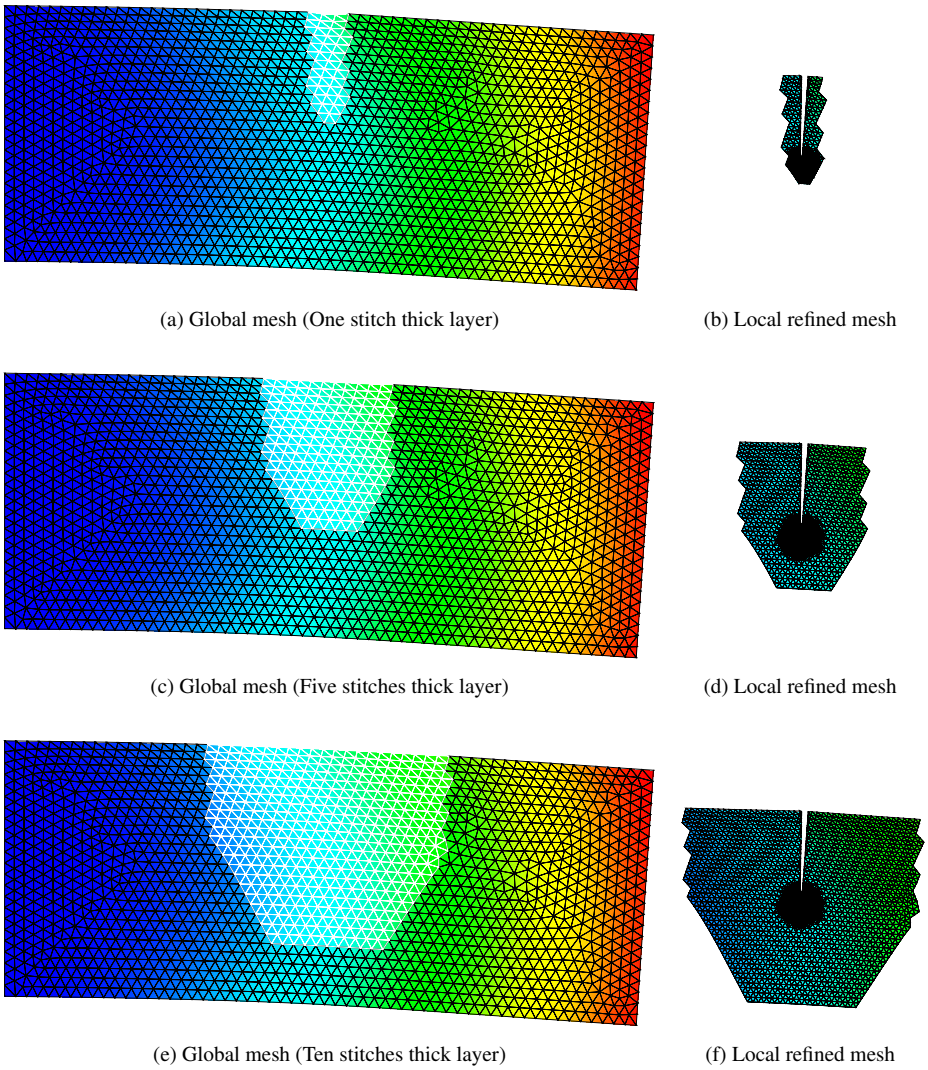

(a) Global mesh (One stitch thick layer) (b) Local refined mesh

(c) Global mesh (Five stitches thick layer) (d) Local refined mesh

(e) Global mesh (Ten stitches thick layer) (f) Local refined mesh

Fig. 6: Patch definition and extend: global stitches selection

3 New advances based on the non-intrusive coupling

3.1 Parallel processing and multi-patch approach

In this part, we seek to extend the non-intrusive coupling method to the multi-patch situation. We give here detailed explanations about the way multi-patching is handled in specific situations (*e.g.* two patches share a common interface), and we provide a MPI based parallel processing method to increase the computational efficiency of the algorithm.
Let us consider a multi-perforated plate subjected to a uniform tension (see Fig. 8).
In order to set up the coupling algorithm, one has to define the following items:

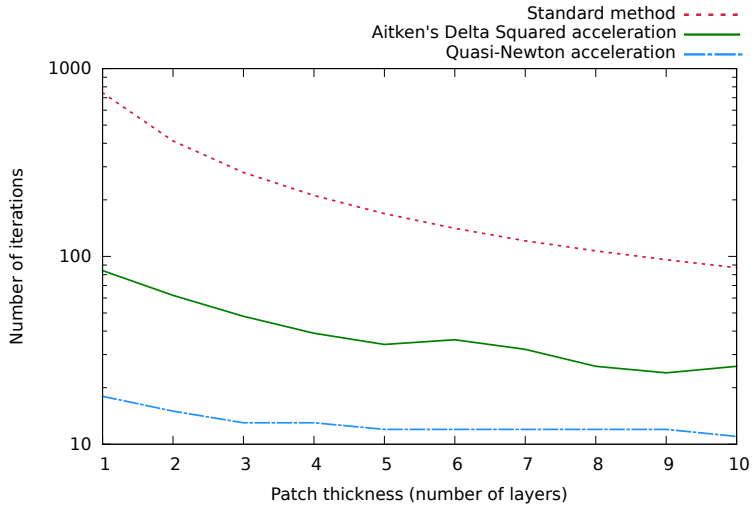

Fig. 7: Convergence speed: patch thickness influence

- The united local domain $\Omega_L = \cup_{i=1}^{6} \Omega_{L,i}$
- The united global fictitious domain $\Omega_{\widetilde{G}} = \cup_{i=1}^{6} \Omega_{\widetilde{G},i}$
- The patches boundary $\Gamma = \cup_{i=1}^{6} \Gamma_i$ with $\Gamma_i = \partial\Omega_{\widetilde{G},i} = \partial\Omega_{L,i}$
- The global domain internal boundary $\Gamma_G = \partial\Omega_G \setminus \partial\Omega = \partial\Omega_{\widetilde{G}}$ so that $\Gamma_G \subset \Gamma$

Note that as soon as all the local models do not share any common interface (*e.g.* if we added a gap between the local domains), then $\Gamma_G = \Gamma$.

Remark: In the previous application (crack propagation), we considered $\Omega_L = \Omega_{\widetilde{G}}$ (*i.e.* as the crack was represented through the XFEM method, the geometrical domain remained unaffected). In the present situation, we allow the local patches to redefine the geometry of the pre-existing global model, so that $\Omega_L \neq \Omega_{\widetilde{G}}$ because of holes [21]. The only required condition is that the interfaces remain coincident (from a geometrical point of view, non-conforming meshes are still handled using the mortar method).

In the non-intrusive coupling context, we consider the global model on $\Omega = \Omega_G \cup \Omega_{\widetilde{G}}$ as a linear elastic material, the holes being absent from the global model on $\Omega_{\widetilde{G}}$. The holes will be represented only through the local models on $(\Omega_{L,i})_{i\in\{1..6\}}$ and elastic-plastic constitutive law will be applied.

From now on, we need to extend the projection operator P to each interface Γ_i, so that $P_i = C_{L,i}^{-1} C_{G,i}$. We will also keep the definition of $\Lambda_G = (K_G U_G - F_G)|_{\Gamma_G}$ and $\Lambda_{\widetilde{G},i} = (K_{\widetilde{G},i} U_{\widetilde{G},i} - F_{\widetilde{G},i})\Big|_{\Gamma_i}$.

Nevertheless, as we consider elastic-plastic (*i.e.* nonlinear) behaviour on the local models, the local reaction reads $\Lambda_{L,i} = \zeta(U_{L,i}, F_{L,i}, \mathbf{X_i})$ where ζ is a nonlinear function computing the reaction forces from the displacement $U_{L,i}$, the right-hand side loading $F_{L,i}$ and the plastic internal variables $\mathbf{X_i}$.

Thus, the multi-patch non-intrusive coupling algorithm can be established, $\mathscr{K}_L$ being the nonlinear local solver.

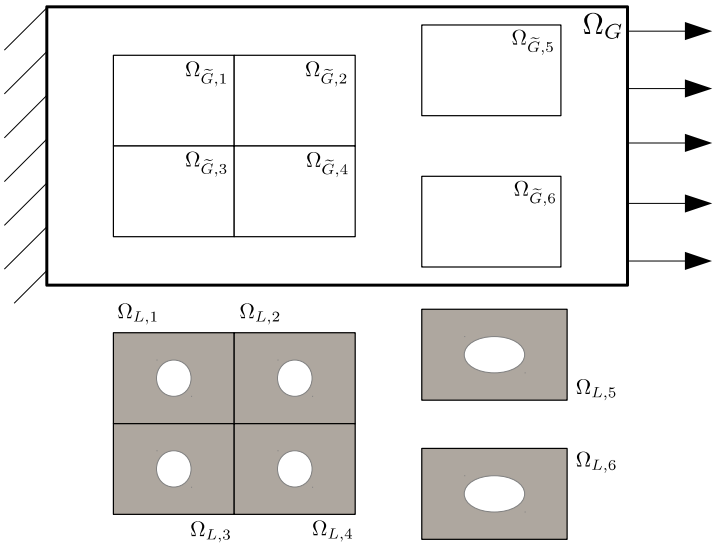

Fig. 8: Situation overview: multi-patch problem

Algorithm 4: Multi-patch coupling – Non-intrusive fixed point solver

Data: ε, $\left(\Lambda^0_{L,i}\right)_{i\in\{1..6\}}$, $\left(\Lambda^0_{\widetilde{G},i}\right)_{i\in\{1..6\}}$

k = 0

while $\eta > \varepsilon$ **do**

Global problem computation

$$KU^{k+1} = F + \sum_{i=1}^{6}\left(-\underline{P}_i^{\top}\,\underline{\Lambda}^k_{L,i} + \underline{\Lambda}^k_{\widetilde{G},i}\right)$$

Local problems computations

$$U^{k+1}_{L,i} = \mathscr{K}_{L,i}\left(P_i\,U^{k+1}\big|_{\Gamma_i}, F_{L,i}, \mathbf{X_i}\right) \qquad \forall i \in \{1..6\}$$

Convergence test

$$\eta = \|\Lambda^{k+1}_G + \sum_{i=1}^{6}\left(P_i^{\top}\,\Lambda^{k+1}_{L,i}\right)\| / \sqrt{\|F_G\|^2 + \sum_{i=1}^{6}\|F_{L,i}\|^2}$$

k = k+1

end

Result: U^k, $\left(U^k_{L,i}\right)_{i\in\{1..6\}}$

As it has been done in the previous section (mono-patch case), the problem can be rewritten in an incremental version as $U^{k+1} = U^k - K^{-1}f(U^k)$. Thus the difference here is that f is a nonlinear operator as soon as the local domains involve elastic-plastic behaviour.

$$f(U^k) = \underline{\Lambda}^k_G + \sum_{i=1}^{6}\left(\underline{P}_i^{\top}\,\underline{\Lambda}^k_{L,i}\right) \tag{50}$$

For the example presented here, we keep the same rectangular domain than the one from the previous example (cracked plate) and the same elastic properties for the global model. The tensile load applied is of magnitude $f_N = 140\ MPa$.
The local models (with holes) are assigned with an elastic-plastic behaviour which elastic

limit is $R_e = 250\ MPa$ and tangent plastic modulus is $E_T = 40\ GPa$ (we assume a linear kinematic hardening law). The local elastic behaviour is also assumed to be the same than the global one before plasticity occurs. It can be seen on Fig. 9 that plasticity occurs at the

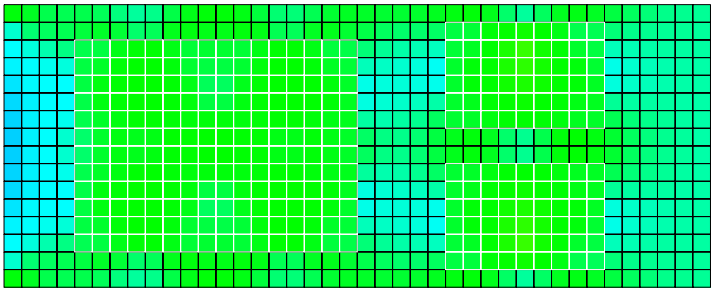

(a) Global elastic solution

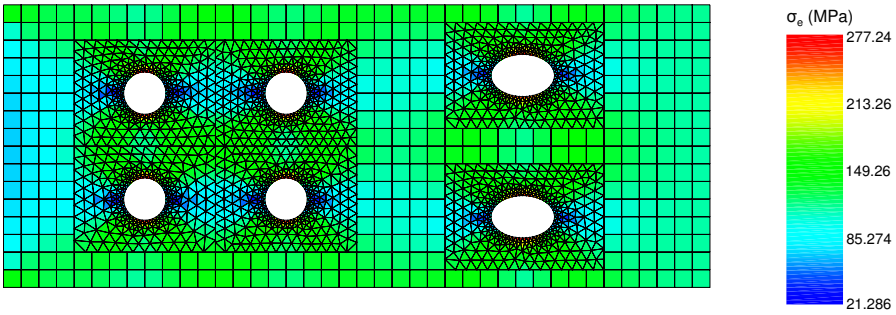

(b) Composite solution (global elastic and local plastic models)

Fig. 9: Non-intrusive multi-patch simulation (Von Mises equivalent stress)

holes edges in the local models. Thus, there is no need to extend the plastic area outside the local patches, which makes global elastic model hypothesis lawful. However if the plasticity was to go out of the local domain (*i.e.* the global Von Mises equivalent stress exceeds the elastic limit), then convergence of the algorithm would not be endangered at all. Still, the computed solution would be false, but such property allows to easily check whether or not the patch extend is well chosen.
Also recall that the global prolonged solution on $\Omega_{\widetilde{G}}$ has no physical meaning and depends only on the algorithm initialisation. The greater stress which can be observed on that area is simply the result of the equilibrium between Ω_G and $\Omega_{\widetilde{G}}$ with prescribed additional forces on Γ.

Last but not least, at iteration i, each local model is independent from the others as it requires only prescribed displacement from the global model. That means we can use parallel processing when computing the local solutions. In our example we considered six local patches, each one being processed by a different thread. One thread was dedicated to the global linear model computing, one to the coupling operations (mainly computing the pro-

jections at the interface) and six to the local models. One of the algorithm most attractive properties here is the fact that only interface displacements and reactions are sent from one thread to the others through MPI (Message Passing Interface) communications. The consequence is the possibility to directly use it within commercial software.

Again, we compare here the Quasi-Newton and Aitken's Delta Squared acceleration meth-

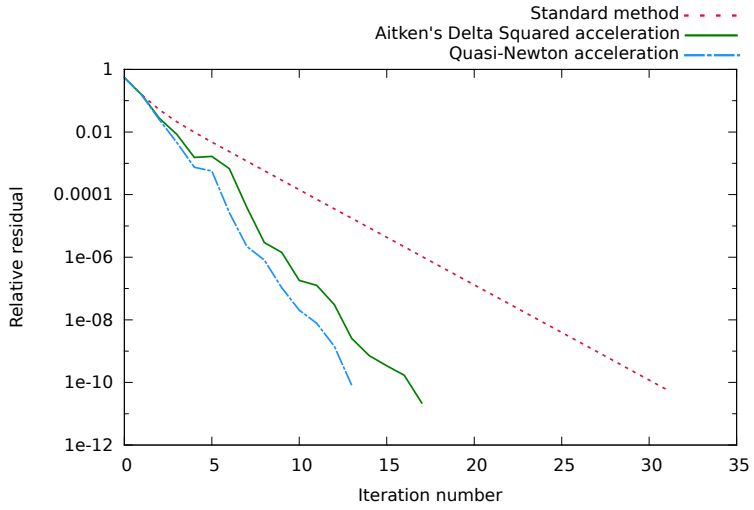

Fig. 10: Multi-patch problem: residual evolution

ods (see Fig. 10). When using the standard method (without any acceleration), the algorithm takes a few iterations to reach the fixed tolerance ($\varepsilon = 10^{-10}$). Still, when dealing with non-linear local models, reducing the number of iterations required at the lowest possible value is wholesome. Both Quasi-Newton and Aitken's Delta Squared accelerations allow to divide by two the required number of iterations with comparable efficiency.
Let us recall that the Aitken formula is much easier to compute than the non-intrusive Symetric Rank One formula. In such a low stiffness gap case, the Aitken's Delta Squared acceleration will provide quite similar convergence speed but will imply less computational overhead than the Quasi-Newton acceleration. Plasticity is thus a typical example for which Aitken's acceleration could be preferred to Quasi-Newton.

Remark: One can notice that, in the present example, some patches share a common interface: such choice is not trivial. Indeed, the algorithm is designed so that data exchange never occurs between local models, but only between the global model and each local ones. When using non-confirming meshes at the interface the global displacement is transferred to the local mesh using a mortar projection. Thus, the global mesh (which is supposed to be coarser than the local mesh) acts as a low-pass filter on the displacement field. It can be seen from Fig. 9b that the global mesh is coarser than the local ones: filtering does occur at the common boundary shared by $\Omega_{L,1}$, $\Omega_{L,2}$, $\Omega_{L,3}$ and $\Omega_{L,4}$, which would not be the case if we used a single patch on $\Omega_{L,1} \cup \Omega_{L,2} \cup \Omega_{L,3} \cup \Omega_{L,4}$ instead of four. If the global mesh is too coarse or if the strain is too sharp near the interface, then the solution may not be

mechanically relevant.

3.2 Local geometric changes, local loading and boundary conditions

In that section, we propose another new advance based upon the non-intrusive coupling method which allows us to extend the method to a more generic application framework. Indeed, in the previous examples, we always considered that the patches were included in the global domain (*i.e.* $\Omega_L \in \Omega$), and that the loading (both Neumann and Dirichlet conditions) was applied to the global domain Ω_G. In fact, nothing prevent us to consider any arbitrary local patches. In the present example (see Fig. 11), we consider a global model whose boundary conditions are badly represented. Then, two patches are set up in order to locally redefine both the geometrical domain Ω and the boundary conditions: the first patch (on the left) redefines the global Dirichlet condition, whereas the second patch (on the right) redefines the global Neumann condition. The most important property of such coupling is the fact that the local model on Ω_L literally substitutes the global model on $\Omega_{\widetilde{G}}$, *i.e.* the boundary conditions applied on the global domain will have absolutely no effect on the composite solution when converged. Thus, the local patches are allowed to partially lay outside the global domain, and the boundary conditions applied to it will overcome the global ones. As for previous examples, we consider the same rectangular domain and the same

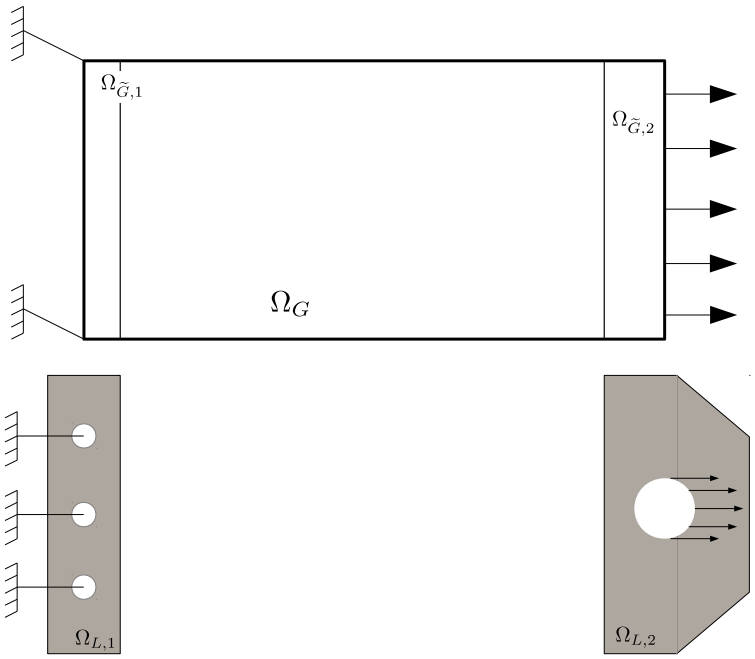

Fig. 11: Situation overview: local loading and boundary conditions

elastic properties for the global model. The global tensile loading is of magnitude 80 *MPa*.

The local models are assigned with the same plastic behaviour than from the previous example (the multi-perforated plate). The local Dirichlet condition is applied through a zero displacement condition at holes edges contained in $\Omega_{L,1}$, and the local Neumann condition is applied with a uniform pressure on the right half-edge of the hole in $\Omega_{L,2}$. The force applied to the local model have the same resultant than the one applied to the global one. This condition is not mandatory at all, but as the local model is here to redefine the rough global boundary conditions, such choice is wholesome.

Moreover, it can be seen from Fig. 12 there is no restriction on the choice of elements (*e.g.*

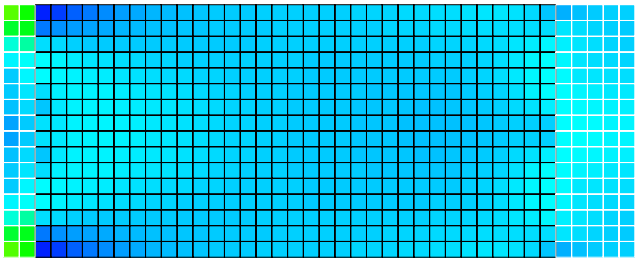

(a) Global solution (Von Mises equivalent stress)

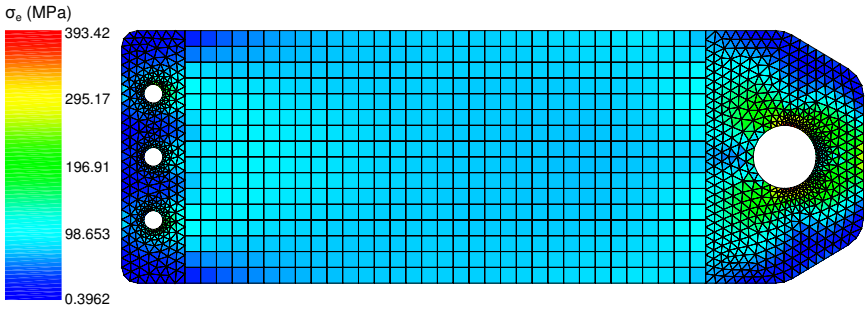

(b) Composite solution (Von Mises equivalent stress)

Fig. 12: Non-intrusive local loading and boundary conditions

P1 / Q1), as we used a mortar gluing at the interface.

In that example, we deliberately forced the local domain $\Omega_{L,1}$ to be stiffer than the global domain $\Omega_{\widetilde{G},1}$ by embedding the three holes (see Fig. 11). The consequence of such a choice is the non-convergence of the algorithm when the initial fixed point algorithm is used alone (see Fig. 13).

Still, it is possible to enforce the stability of the algorithm using relaxation with a constant parameter ω [21]. We used here $\omega = 0.115$ which has been found empirically to be the optimal relaxation parameter, but ω can also be optimised during the first iterations thanks to a power-type method [21]. Still, it may be noted that Aitken's dynamic relaxation provides a faster convergence. Nevertheless, it can be seen again that the Quasi-Newton SR1 update remains the best option when the local patches strongly affect the global mechanical behaviour.

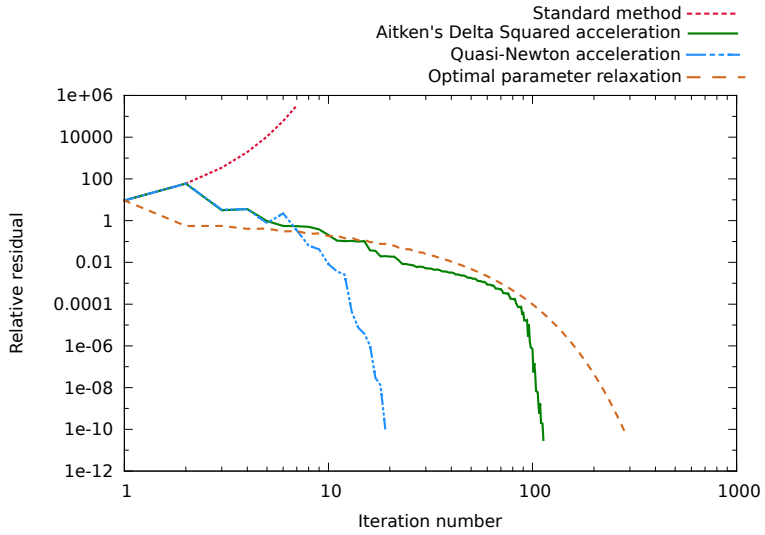

Fig. 13: Local loading problem: residual evolution

Such non-intrusive geometric changes may remind the reader of the fictitious domain methods. Actually, one could use fictitious domain principle to take into account local geometric changes in an even less intrusive way, *i.e.* allowing non-coincident interfaces [44, 4]. Indeed, in the present paper, we stand to coincident interfaces, and consider only the mortar method in order to compute the interface projection.

3.3 Local contact problem

The last example of non-intrusive coupling we give here is a three-dimensional contact problem. Such nonlinear behaviour is commonly considered in structural analysis, mostly when dealing with assemblies (*e.g.* bolted structures). Then, to dissociate the local contact area from the global structure when computing such problems is of great interest for many engineers.
In the present example (see Fig. 14) we consider an elastic body ($200 \times 80 \times 20$ *mm*, $E = 40$ *MPa*, $\nu = 0.45$) as the global model. Then we want to investigate a contact condition with a rigid spindle ($E = 200$ *GPa*, $\nu = 0.3$, with radius $r = 10$ *mm*) at the center of the body (the local model is constituted with the rigid spindle and a part of the elastic body). Tensile loading is applied to the boundary of the plate with magnitude $f_N = 1$ *MPa*, the spindle ends being assigned with zero displacement. Actually, if one had to deal with bolted structures, a local patch could be considered for each bolt (*i.e.* each contact area). Indeed, solving a multi-contact problem in a monolithic way is not an easy task as convergence properties of the nonlinear solvers are worsened by the increase of contact surfaces number. Then, using non-intrusive coupling allows to dissociate each local contact problem, and is expected to lead to an easier convergence of the nonlinear solvers. Here, Fig. 16 shows the greater efficiency of the Quasi-Newton update against the Aitken's acceleration. Note that, in that case, we could not use the coupling algorithm in its standard formulation as it led

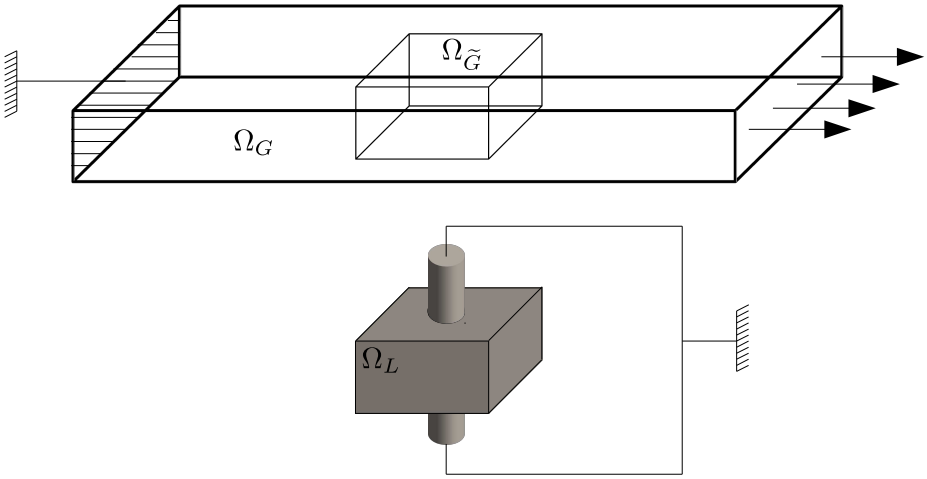

Fig. 14: Situation overview: local contact problem

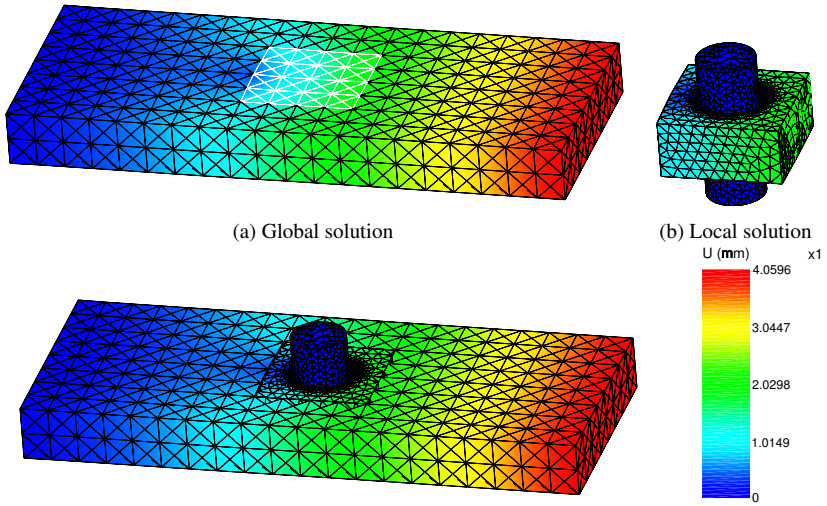

(a) Global solution

(b) Local solution

(c) Composite solution

Fig. 15: Non-intrusive local contact simulation

to very quick divergence, preventing the local nonlinear solver to convergence after the first two global/local iterations.

3.4 Nonlinear local patches: caution

Special attention should be given to local nonlinear problems. Indeed, the local Dirichlet problem is computed using global displacement as boundary condition, which is by definition far from the final solution during the firsts global/local iterations. In some cases, such

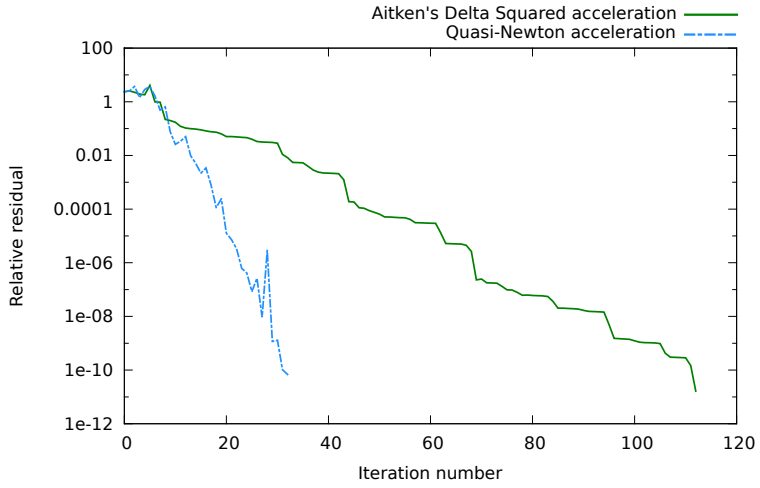

Fig. 16: Local contact problem: residual evolution

imposed displacement appears to be too severe, preventing the local nonlinear solver to converge, or at least worsening the convergence properties. Such situation mostly occurs when the local patch redefine the geometry or the structure loading, *e.g.* we embed the holes in Fig. 11 or add a contact condition in Fig. 14. Then, a possible workaround is to use a local linear model for the firsts global/local iterations (*i.e.* compute a predicted initial solution), before switching to the desired nonlinear model. For instance, when dealing with local plasticity, using a linear elastic law during the firsts global/local iterations allows to approximate the actual solution at lower cost. Then, when switching to elasto-plastic law, a few more (that will depend on the situation considered) global/local iterations will be required in order to achieve the convergence. In the same way, when dealing with the local contact problem, one can replace the contact condition by a mesh gluing during the first global/local iterations. In a general manner, $U^0 = K^{-1}F$ is a "bad" starting point from which convergence of the global/local iterative algorithm is not guaranteed when dealing with local nonlinear models. Thus, computing a "good" starting point U^0 is essential. Note that in the above examples, we used such linear initialisation only for the contact problem, while we did not need it for all the others examples.
Of course, computing such predicted solution U^0 is not always an easy task, and one cannot hope such trick to be efficient for every encountered problem. Another workaround would be to apply the global loading F in an incremental manner and apply the global/local iterative algorithm for each load increment, though it would result in larger computation time.

4 A novel domain decomposition method based on non-intrusive coupling

In this section, an attempt is made to extend the concept of non-intrusive coupling to nonlinear domain decomposition (DD). In fact, domain decomposition methods and global/local methods share several similarities: they are both based upon multi-domain equilibrium problem, and both allow to connect non-conforming models.
Historically, domain decomposition relied on overlapping partition of the domain, such as Schwarz methods [60, 32]. Non overlapping approaches were preferred for implementation

issues, but also because they better correspond to mechanical assemblies. The principle of dual domain decomposition (like Finite Element Tearing and Interconnecting, FETI [28]) is to enforce interface reaction equilibrium, while seeking to reach displacement equality. On the contrary, primal domain decomposition enforces displacement equality at the interface, while converging toward reaction equilibrium throughout the iterative process. Mixed approaches (like Large Time Increment Method LATIN [56] or FETI-2LM [79]) gather both primal and dual principle by enforcing a linear combination of displacement and effort at the interface (*i.e.* Fourier-Robin condition). A hybrid method has also been developped which unifies primal and dual approaches [38]. It allows the use of a primal method on a set of degrees of freedom and a dual method on the remainder, which may be relevant for multiphysic problems.
Initial methods [56, 28] suffered from several drawbacks among which bad scalability. Many improvements have therefore been made to allow for analysing efficiently large number of sub-domains. First, the primal approach, referred to as Balancing Domain Decomposition, BDD [62], introduced a kind of coarse problem associated to the use of a dual preconditionner. A coarse problem based on the rigid body modes of floating subdomains is also introduced in FETI [29]. In a similar way, a *macro* problem is used in the mixed LATIN method [59] to ensure the equilibrium of resultant moments and forces at interfaces. These coarse problems provide better scalability properties to the domain decomposition methods. Special treatments of subdomain corners, FETI-DP [30] and BDDC [26, 63] was shown to improve even further the convergence and scalability properties over standard FETI and BDD methods. Finally, in the case of time dependant problems, a space-time macro problem can also been used to make space-time decomposition methods scalable [72].
nonlinear problems can also be solved by domain decomposition methods. Most often, the DD solver is used to solve the linear predictions arising from a Newton-type algorithm. They are known as Newton-Krylov-Shur methods (NKS). However, in the case of localised nonlinearities, this algorithm is not the most effective. nonlinear domain decomposition methods with nonlinear localisation problems have been proposed [23, 75, 6, 5]. It was shown that such approaches were more efficient in this case, since they focus the computational efforts on the local nonlinearities which reduces the number of global iterations. This is also the basic idea of the LATIN method [56, 57, 72]. However, the main drawback of these methods is that they have a high degree of intrusiveness. So far, they have been implemented only in research codes adapted for academic test cases, but still engineers face difficulties to use it on representative applications. Conversely, industrial partners would favour developments within commercial (certified) software.
In the following, we propose to use the non-intrusive coupling as a scalable nonlinear domain decomposition method. The idea is to consider a mesh partition of the global structure, and use each part as a local model, the global model being thus completely covered by local patches. Then, the global/local non-intrusive coupling algorithm is used in the same way is has been done in the previous example (see Fig. 17 and 18):

- a global linear (*e.g.* linear elasticity) computation is completed on the full structure, with additional reactions forces at the interface
- local nonlinear (*e.g.* plasticity) computation is completed on each sub-domain, with prescribed displacement on the interface.

Compared to classical domain decomposition methods, such method requires to compute a linear problem on the full structure at each iteration in addition to the local nonlinear computation. Nevertheless, such overhead can be neglected beside the nonlinear computation cost. Moreover, such linear computation could also be achieve using a domain-decomposition

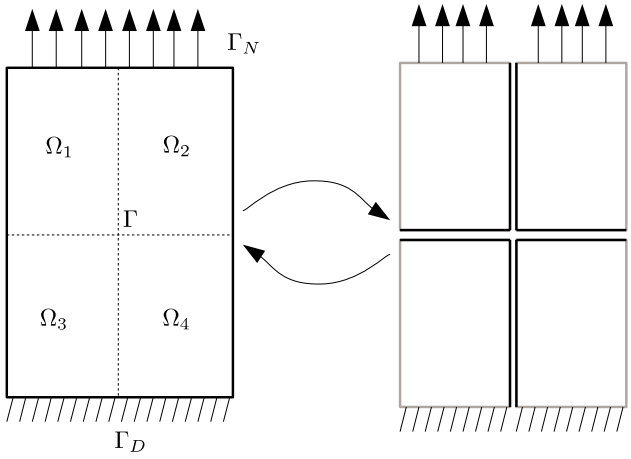

Fig. 17: Non-intrusive domain decomposition

based solver (*e.g.* using the same mesh partition), possibly with model reduction.
In addition to its non-intrusive character which makes it easy to use (even in a sequential and black box software), such a method have the following advantages:

- The global linear problem plays the role of a physically relevant macro (or coarse) problem that was used in FETI-DP [30], BDD-C [26], and the multiscale LATIN method [59]. As it will be shown in the examples below, such a coarse problem provide good scalability properties.
- The independant local problems embed the nonlinearities like the nonlinear localisation solvers do [23, 75]. This makes the algorithm efficient even in the case of localised nonlinearities.
- When domain decomposition is used as a parallel solver, interfaces are most of time mesh-conforming. Nevertheless, nothing prevent the use of non-conforming interfaces [2, 71, 45, 17] especially when one is dealing with heterogeneous models. As shown before, the above presented non-intrusive domain coupling solver is also ready for incompatible meshes at interface.
- The method can be seen as a dual domain decomposition based upon an asymmetric Neumann-Dirichlet algorithm. Due to that Neumann-Dirichlet formulation, one is not constrained by floating substructures.

As a purpose of illustration, we consider here the example of a planetary gear carrier (diameter $d = 155$ *mm*). A torque is applied to the central axe ($C = 50$ *kNm*), and a zero displacement condition is applied to the gear carrier sideboards (see Fig. 19). The mesh (about $70,000$ degrees of freedom) has been divided into twelve parts (see Fig. 20). We then applied the non-intrusive coupling algorithm, *i.e.* solving alternately a linear elastic problem on the full mesh, and an elastic-plastic problem on each of the twelve sub-domains. In that case, the local meshes are just a part of the global mesh, so that no mortar method is needed here (still we could easily handle a non-conforming situation). Fig. 21 shows the Von Mises equivalent stress when converged. As usually, the same acceleration techniques can be applied in the present case, allowing for substantial iteration saving when using the iterative algorithm (with relative tolerance $\varepsilon = 10^{-10}$, see Fig. 22). As expected, both Quasi-Newton and Aitken updates provide a significant acceleration of the algorithm with quite similar

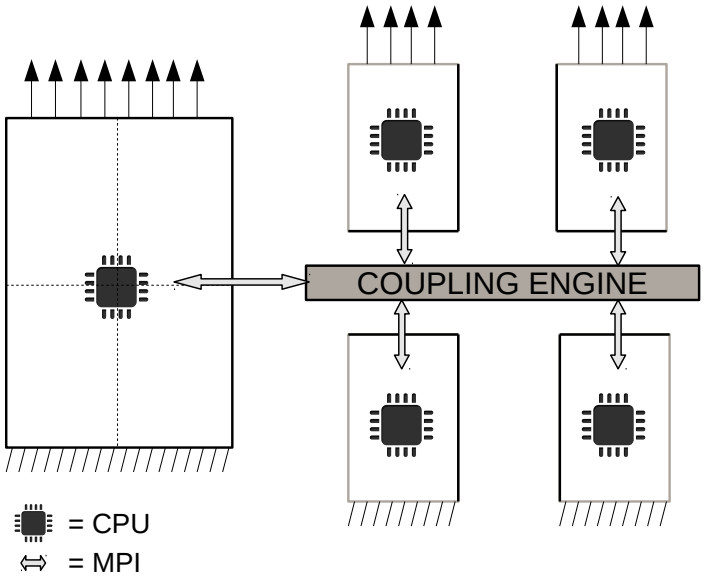

Fig. 18: Non-intrusive MPI communication

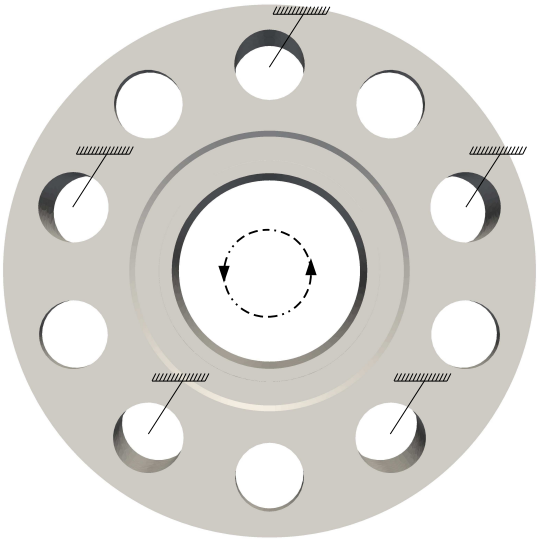

Fig. 19: Situation overview: planetary gear carrier

efficiency (the Quasi-Newton acceleration still proves to be the better method in terms of iteration number reduction).

Let us now study the effect of the number of sub-domains. We thus did the same computation considering several sub-domains numbers, from two to sixty. The most important

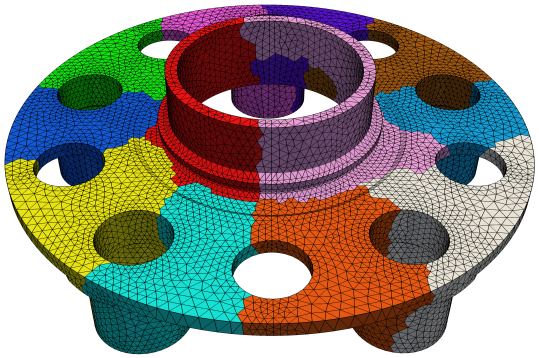

Fig. 20: Planetary gear carrier: mesh partition (twelve sub-domains)

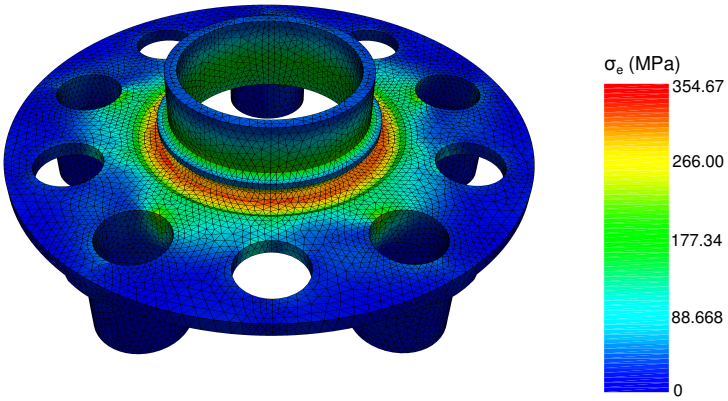

Fig. 21: Planetary gear carrier: Von Mises equivalent stress

result about the application of the non-intrusive coupling to domain decomposition is illustrated by Fig. 23. Indeed as one can see, when using acceleration techniques, the number of iterations required to reach a fixed tolerance nearly does not depend on the number of sub-domains considered.
Actually, in standard methods, each sub-domain shares data only with its neighbours, which makes the algorithm not directly scalable. Using non-intrusive coupling algorithm, each sub-domain shares data with the global model only, allowing for instantaneous propagation of the information (stress residual). The consequence is the scalability of the method.

5 Conclusion

We proposed in this paper a detailed review of the non-intrusive coupling algorithm. Such algorithm allows for taking into account localised details into an existing finite element model,

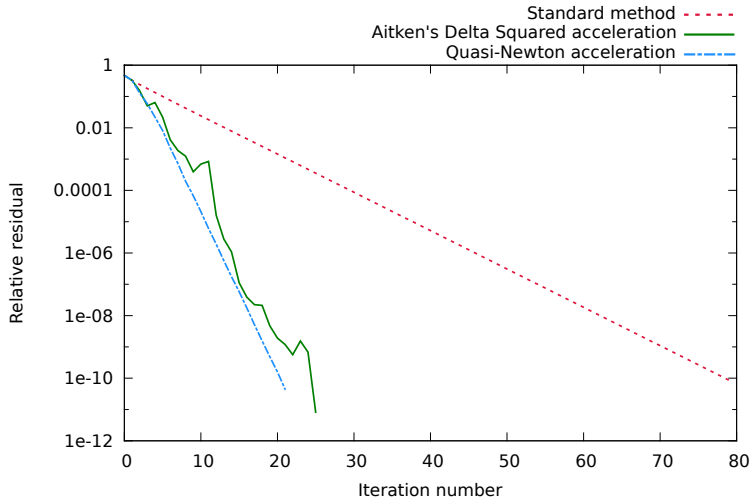

Fig. 22: Domain decomposition: residual evolution (twelve sub-domains)

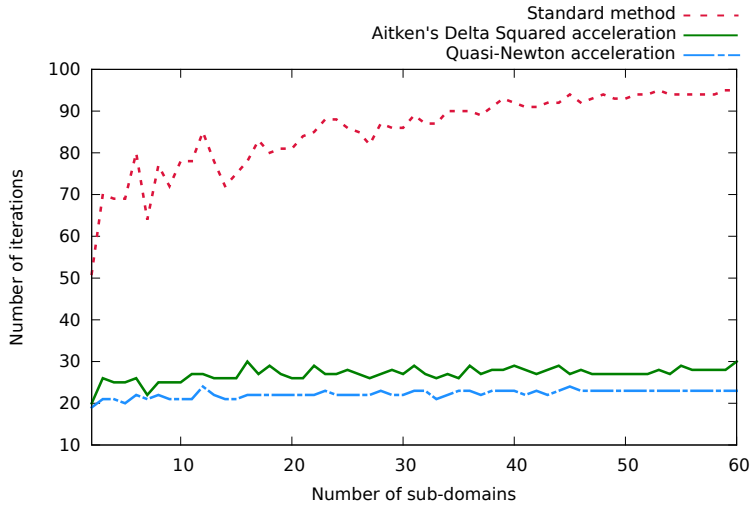

Fig. 23: Domain decomposition: scalability

without actually modifying its corresponding numerical operator. We also investigated two existing improvements (Quasi-Newton update and Aitken dynamic relaxation), allowing for better efficiency of the algorithm, while focusing on the relative benefits of both processes: we showed the Quasi-Newton acceleration to be more efficient than the Aitken dynamic relaxation in all situations, while requiring slightly more computational overhead.
We also extended the coupling method and algorithm to various situations and advanced applications we consider useful in both research and engineering context: crack propagation, multi-patching, boundary condition modification, geometric changes and contact. Additionally to those extensions, we setted up a flexible and efficient implementation of the coupling,

based upon the Message Passing Library (MPI) granting a universal way to use non-intrusive coupling in a given software environment.
We finally proposed a novel domain decomposition method based upon the the non-intrusive coupling algorithm, intended to large scale nonlinear analysis, and showed its scalability. Such novel method has several advantages:

- the possibility to use sequential commercial software thanks to the non-intrusiveness property of the algorithm,
- the use of a global model provides scalability of the algorithm and releases one from taking care of floating sub-structures, moreover such global model is kept unmodified whatever happens to the sub-structures and the interfaces,
- non-conforming meshes at the interface between two sub-structures are easily handled, allowing for an easy and flexible design of the model,
- the algorithm provides a straightforward localisation of the nonlinearities, and thus allows to reduce the overall number of iterations.

As a short term perspective, such domain decomposition method is expected to be highly optimised in order to make it usable on very large models (millions of degrees of freedom). Moreover, the non-intrusive coupling procedure remains under constant investigation in order to improve its integration into common nonlinear Newton-Krylov-Schur (NKS) solvers.

Acknowledgements The authors would like to acknowledge the financial support of the Agence Nationale de la Recherche under Grant ICARE ANR-12-MONU-0002.
Dr. Crozes (Airbus Group Innovation) is also acknowledged for providing the planetary gear carrier model.

A Non-intrusive coupling program

Jointly to this paper, the complete code used to run example from §3.2 is also provided. It can be downloaded from [1].
The overall code is organised as follow:

- the global model is computed by *Code_Aster* using *structure.comm*, *global.py* and *optimisation.py* files,
- the local model is computed by *Code_Aster* using *patch.comm*, *global.py* and *optimisation.py*
- the interface coupling is achieved by a *Python* script using *coupling_engine.py* and *coupleur.py* files,
- the finite element meshes have been saved into the *mesh.med* file,
- the *Code_Aster* global and local programs configuration files are *global.export* and *local.export* respectively (such files have to be adapted to the version of *Code_Aster* used, the one used here is *STA11.4*).

Each program (global, local and coupling engine) have to be launched separately (see file *run.sh*) with the *mpirun* command as we use MPI communications between them for the interface data exchange (see Fig 24). In fact, the MPI communication is based upon a client–server model, so that there is no need for a parallel version of *Code_Aster*. Parallelism is thus ensured by the simultaneous run of several sequential instances.

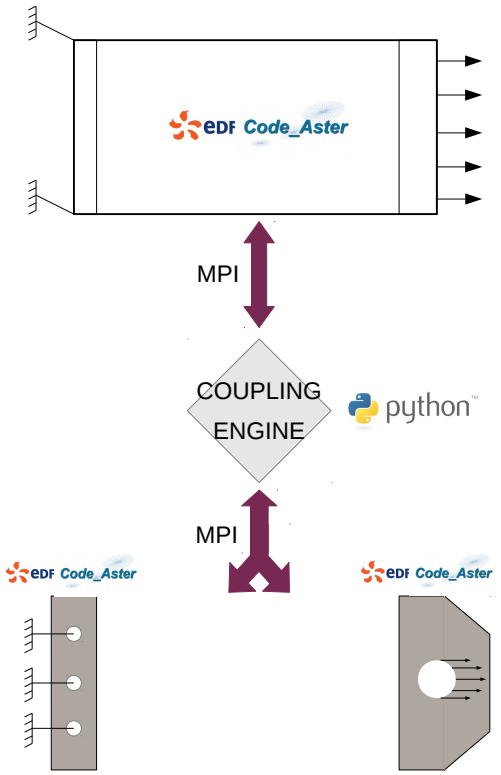

Fig. 24: Non-intrusive coupling: MPI communication between *Code_Aster* and *Python*

References

1. Agence Nationale de la Recherche (2014) Icare project. URL http://www.institut-clement-ader.org/icare/
2. Agouzal A, Thomas JM (1995) Une méthode d'éléments finis hybrides en décomposition de domaines. ESAIM: Mathematical Modelling and Numerical Analysis 29:749–764
3. Akgün MA, Garcelon JH, Haftka RT (2001) Fast exact linear and non-linear structural reanalysis and the Sherman–Morrison–Woodbury formulas. International Journal for Numerical Methods in Engineering 50(7):1587–1606
4. Amdouni S, Moakher M, Renard Y (2014) A local projection stabilization of fictitious domain method for elliptic boundary value problems. Applied Numerical Mathematics 76:60–75
5. Barrière L (2014) Stratégies de calcul intensif pour la simulation du post-flambement local des grandes structures composites raidies aéronautiques. PhD Thesis, INSA de Toulouse
6. Barrière L, Marguet S, Castanié B, Cresta P, Passieux JC (2013) An adaptive model reduction strategy for post-buckling analysis of stiffened structures. Thin-Walled Structures 73:81–93

7. Becker R, Hansbo P, Stenberg R (2003) A finite element method for domain decomposition with non-matching grids. ESAIM: Mathematical Modelling and Numerical Analysis 37(02):209–225
8. Belgacem FB (1999) The mortar finite element method with Lagrange multipliers. Numerische Mathematik 84(2):173–197
9. Ben Dhia H, Jamond O (2010) On the use of XFEM within the Arlequin framework for the simulation of crack propagation. Computer Methods in Applied Mechanics and Engineering 199(21):1403–1414
10. Ben Dhia H, Rateau G (2005) The Arlequin method as a flexible engineering design tool. International Journal for Numerical Methods in Engineering 62(11):1442–1462
11. Ben Dhia H, Elkhodja N, Roux FX (2008) Multimodeling of multi-alterated structures in the Arlequin framework: Solution with a Domain-Decomposition solver. European Journal of Computational Mechanics 17(5–7):969–980
12. Bernardi C, Maday Y, Patera AT (1994) A new nonconforming approach to domain decomposition: the Mortar element method. Nonlinear partial differential equations and their applications, Collège de France Seminar XI, H Brezis and JL Lions (Eds) pp 13–51
13. Bernardi C, Maday Y, Rapetti F (2005) Basics and some applications of the mortar element method. GAMM-Mitteilungen 28(2):97–123
14. Bettinotti O, Allix O, Malherbe B (2014) A coupling strategy for adaptive local refinement in space and time with a fixed global model in explicit dynamics. Computational Mechanics 53(4):561–574
15. Bjorstad PE, Widlund OB (1986) Iterative methods for the solution of elliptic problems on regions partitioned into substructures. SIAM Journal on Numerical Analysis 23(6):1097–1120
16. Brancherie D, Dambrine M, Vial G, Villon P (2008) Effect of surface defects on structure failure: a two-scale approach. European Journal of Computational Mechanics 17(5-7):613–624
17. Brezzi F, Marini LD (2005) The three-field formulation for elasticity problems. GAMM-Mitteilungen 28(1):124–153
18. Chahine E, Laborde P, Renard Y (2008) Spider-XFEM, an extended finite element variant for partially unknown crack-tip displacement. European Journal of Computational Mechanics 17(5-7):625–636
19. Chahine E, Laborde P, Renard Y (2009) A reduced basis enrichment for the eXtended finite element method. Mathematical Modelling of Natural Phenomena 4(01):88–105
20. Chantrait T, Rannou J, Gravouil A (2014) Low intrusive coupling of implicit and explicit time integration schemes for structural dynamics: Application to low energy impacts on composite structures. Finite Elements in Analysis and Design 86:23–33
21. Chevreuil M, Nouy A, Safatly E (2013) A multiscale method with patch for the solution of stochastic partial differential equations with localized uncertainties. Computer Methods in Applied Mechanics and Engineering 255:255–274
22. Conn AR, Gould NIM, Toint PL (1991) Convergence of quasi-newton matrices generated by the symmetric rank one update. Mathematical Programming 50(1-3):177–195
23. Cresta P, Allix O, Rey C, Guinard S (2007) Nonlinear localization strategies for domain decomposition methods: Application to post-buckling analyses. Computer Methods in Applied Mechanics and Engineering 196(8):1436–1446
24. Daghia F, Ladevèze P (2012) A micro–meso computational strategy for the prediction of the damage and failure of laminates. Composite Structures 94(12):3644–3653
25. Daridon L, Dureisseix D, Garcia S, Pagano S (2011) Changement d'échelles et zoom structural. In: 10e colloque national en calcul des structures, Giens, France

26. Dohrmann C (2003) A Preconditioner for Substructuring Based on Constrained Energy Minimization. SIAM Journal on Scientific Computing 25(1):246–258
27. Duarte CA, Kim DJ (2008) Analysis and applications of a generalized finite element method with global–local enrichment functions. Computer Methods in Applied Mechanics and Engineering 197(6–8):487–504
28. Farhat C, Roux FX (1991) A method of finite element tearing and interconnecting and its parallel solution algorithm. International Journal for Numerical Methods in Engineering 32(6):1205–1227
29. Farhat C, Mandel J, Roux FX (1994) Optimal convergence properties of the FETI domain decomposition method. Computer Methods in Applied Mechanics and Engineering 115(3–4):365–385
30. Farhat C, Lesoinne M, LeTallec P, Pierson K, Rixen D (2001) FETI-DP: a dual–primal unified FETI method – Part I: A faster alternative to the two-level FETI method. International Journal for Numerical Methods in Engineering 50(7):1523–1544
31. Fritz A, Hüeber S, Wohlmuth B (2004) A comparison of mortar and Nitsche techniques for linear elasticity. Calcolo 41(3):115–137
32. Gander MJ (2008) Schwarz Methods over the Course of Time. Electronic Transactions on Numerical Analysis 31:228–255
33. Gander MJ, Japhet C (2013) Algorithm 932: PANG: Software for Nonmatching Grid Projections in 2D and 3D with Linear Complexity. ACM Transactions on Mathematical Software 40(1):1–25
34. Gendre L, Allix O, Gosselet P, Comte F (2009) Non-intrusive and exact global/local techniques for structural problems with local plasticity. Computational Mechanics 44(2):233–245
35. Gendre L, Allix O, Gosselet P (2011) A two-scale approximation of the Schur complement and its use for non-intrusive coupling. International Journal for Numerical Methods in Engineering 87(9):889–905
36. Gerstenberger A, Tuminaro RS (2013) An algebraic multigrid approach to solve extended finite element method based fracture problems. International Journal for Numerical Methods in Engineering 94(3):248–272
37. Glowinski R, Le Tallec P (1990) Augmented lagrangian interpretation of the nonoverlapping Schwartz alternating method. Philadelphia, SIAM, pp 224–231
38. Gosselet P, Rey C (2006) Non-overlapping domain decomposition methods in structural mechanics. Archives of Computational Methods in Engineering 13(4):515–572
39. Guguin G, Allix O, Gosselet P, Guinard S (2014) Nonintrusive coupling of 3D and 2D laminated composite models based on finite element 3D recovery. International Journal for Numerical Methods in Engineering 98(5):324–343
40. Guidault PA, Allix O, Champaney L, Cornuault C (2008) A multiscale extended finite element method for crack propagation. Computer Methods in Applied Mechanics and Engineering 197(5):381–399
41. Gupta P, Pereira J, Kim DJ, Duarte C, Eason T (2012) Analysis of three-dimensional fracture mechanics problems: A non-intrusive approach using a generalized finite element method. Engineering Fracture Mechanics 90:41–64
42. Hansbo A, Hansbo P (2002) An unfitted finite element method, based on Nitsche's method, for elliptic interface problems. Computer Methods in Applied Mechanics and Engineering 191(47-48):5537–5552
43. Hansbo A, Hansbo P, Larson MG (2003) A finite element method on composite grids based on Nitsche's method. ESAIM: Mathematical Modelling and Numerical Analysis 37(03):495–514

44. Hautefeuille M, Annavarapu C, Dolbow JE (2012) Robust imposition of Dirichlet boundary conditions on embedded surfaces. International Journal for Numerical Methods in Engineering 90(1):40–64
45. Herry B, Di Valentin L, Combescure A (2002) An approach to the connection between subdomains with non-matching meshes for transient mechanical analysis. International Journal for Numerical Methods in Engineering 55(8):973–1003
46. Hirai I, Wang BP, Pilkey WD (1984) An efficient zooming method for finite element analysis. International Journal for Numerical Methods in Engineering 20(9):1671–1683
47. Hughes TJR (1995) Multiscale phenomena: Green's functions, the Dirichlet-to-Neumann formulation, subgrid scale models, bubbles and the origins of stabilized methods. Computer Methods in Applied Mechanics and Engineering 127(1–4):387–401
48. Ibrahimbegović A, Markovič D (2003) Strong coupling methods in multi-phase and multi-scale modeling of inelastic behavior of heterogeneous structures. Computer Methods in Applied Mechanics and Engineering 192(28–30):3089–3107
49. Irons BM, Tuck RC (1969) A version of the Aitken accelerator for computer iteration. International Journal for Numerical Methods in Engineering 1(3):275–277
50. Kelley CT, Sachs EW (1998) Local Convergence of the Symmetric Rank-One Iteration. Computational Optimization and Applications 9(1):43–63
51. Khalfan HF, Byrd RH, Schnabel RB (1993) A Theoretical and Experimental Study of the Symmetric Rank-One Update. SIAM Journal on Optimization 3(1):1–24
52. Khiyabani FM, Hassan MA, Leong WJ (2010) Convergence of Symmetric Rank-One method based on Modified Quasi-Newton equation. Journal of Mathematics Research 2(3):97–102
53. Kim DJ, Duarte CA, Proenca SP (2012) A generalized finite element method with global-local enrichment functions for confined plasticity problems. Computational Mechanics 50(5):563–578
54. Küttler U, Wall WA (2008) Fixed-point fluid–structure interaction solvers with dynamic relaxation. Computational Mechanics 43(1):61–72
55. Laborde P, Lozinski A (in progress) Numerical zoom for multi-scale and multi-model problems
56. Ladeveze P (1985) Sur une famille d'algorithmes en mécanique des structures. Comptes-rendus des séances de l'Académie des sciences Série 2, Mécanique-physique, chimie, sciences de l'univers, sciences de la terre 300(2):41–44
57. Ladeveze P, Nouy A, Loiseau O (2002) A multiscale computational approach for contact problems. Computer Methods in Applied Mechanics and Engineering 191(43):4869–4891
58. Ladevèze P, Dureisseix D (1999) Une nouvelle stratégie de calcul micro/macro en mécanique des structures. Comptes Rendus de l'Académie des Sciences - Series IIB - Mechanics-Physics-Astronomy 327(12):1237–1244
59. Ladevèze P, Loiseau O, Dureisseix D (2001) A micro–macro and parallel computational strategy for highly heterogeneous structures. International Journal for Numerical Methods in Engineering 52(1–2):121–138
60. Lions PL (1987) On the Schwarz method. In: Domain Decomposition Methods for Partial Differential Equations, R. Glowinski, G.H. Golub, G.A. Meurant, J. Périaux (Eds.), Paris, France
61. Liu YJ, Sun Q, Fan XL (2014) A non-intrusive global/local algorithm with non-matching interface: Derivation and numerical validation. Computer Methods in Applied Mechanics and Engineering 277:81–103

62. Mandel J (1993) Balancing Domain Decomposition. Communications in Numerical Methods in Engineering 9:233–241
63. Mandel J, Dohrmann CR (2003) Convergence of a balancing domain decomposition by constraints and energy minimization. Numerical Linear Algebra with Applications 10(7):639–659
64. Mao KM, Sun CT (1991) A refined global-local finite element analysis method. International Journal for Numerical Methods in Engineering 32(1):29–43
65. Massing A, Larson MG, Logg A (2012) Efficient implementation of finite element methods on non-matching and overlapping meshes in 3D. arXiv preprint
66. Melenk J, Babuška I (1996) The partition of unity finite element method: Basic theory and applications. Computer Methods in Applied Mechanics and Engineering 139(1–4):289–314
67. Moës N, Dolbow J, Belytschko T (1999) A finite element method for crack growth without remeshing. International Journal for Numerical Methods in Engineering 46(1):131–150
68. Nguyen VP, Kerfriden P, Claus S, Bordas SPA (2013) Nitsche's method for mixed dimensional analysis: conforming and non-conforming continuum-beam and continuum-plate coupling. arXiv preprint
69. Nocedal J, Wright S (2006) Numerical Optimization, 2nd edn. Springer, New York
70. Oden JT, Vemaganti K, Moës N (1999) Hierarchical modeling of heterogeneous solids. Computer Methods in Applied Mechanics and Engineering 172(1–4):3–25
71. Park KC, Felippa CA (2000) A variational principle for the formulation of partitioned structural systems. International Journal for Numerical Methods in Engineering 47(1–3):395–418
72. Passieux JC, Ladevèze P, Néron D (2010) A scalable time–space multiscale domain decomposition method: adaptive time scale separation. Computational Mechanics 46(4):621–633
73. Passieux JC, Gravouil A, Réthoré J, Baietto MC (2011) Direct estimation of generalized stress intensity factors using a three-scale concurrent multigrid XFEM. International Journal for Numerical Methods in Engineering 85(13):1648–1666
74. Passieux JC, Réthoré J, Gravouil A, Baietto MC (2013) Local/global non-intrusive crack propagation simulation using a multigrid XFEM solver. Computational Mechanics 52(6):1381–1393
75. Pebrel J, Rey C, Gosselet P (2008) A nonlinear dual domain decomposition method : application to structural problems with damage. International Journal for Multiscale Computational Engineering 6(3):251–262
76. Picasso M, Rappaz J, Rezzonico V (2008) Multiscale algorithm with patches of finite elements. Communications in Numerical Methods in Engineering 24(6):477–491
77. Pironneau OP, Lozinski A (2011) Numerical Zoom for localized Multiscales. Numerical Methods for Partial Differential Equations 27:197–207
78. Rannou J, Gravouil A, Baïetto-Dubourg MC (2009) A local multigrid XFEM strategy for 3D crack propagation. International Journal for Numerical Methods in Engineering 77(4):581–600
79. Roux FX (2009) A FETI-2lm method for non-matching grids. In: Domain Decomposition Methods in Science and Engineering XVIII, no. 70 in Lecture Notes in Computational Science and Engineering, Springer Berlin Heidelberg, pp 121–128
80. Réthoré J, Roux S, Hild F (2010) Hybrid analytical and extended finite element method (HAX-FEM): A new enrichment procedure for cracked solids. International Journal for Numerical Methods in Engineering 81(3):269–285

81. Strouboulis T, Copps K, Babuška I (2001) The generalized finite element method. Computer Methods in Applied Mechanics and Engineering 190(32–33):4081–4193
82. Whitcomb JD (1991) Iterative global/local finite element analysis. Computers & Structures 40(4):1027–1031
83. Wohlmuth BI (2000) A Mortar Finite Element Method Using Dual Spaces for the Lagrange Multiplier. SIAM Journal on Numerical Analysis 38(3):989–1012
84. Wohlmuth BI (2003) A Comparison of Dual Lagrange Multiplier Spaces for Mortar Finite Element Discretizations. ESAIM: Mathematical Modelling and Numerical Analysis 36(6):995–1012
85. Wyart E, Duflot M, Coulon D, Martiny P, Pardoen T, Remacle JF, Lani F (2008) Substructuring FE–XFE approaches applied to three-dimensional crack propagation. Journal of Computational and Applied Mathematics 215(2):626–638
86. Wyart E, Coulon D, Pardoen T, Remacle J, Lani F (2009) Application of the substructured finite element/extended finite element method (s-FE/XFE) to the analysis of cracks in aircraft thin walled structures. Engineering Fracture Mechanics 76(1):44–58
87. Zohdi TI, Oden JT, Rodin GJ (1996) Hierarchical modeling of heterogeneous bodies. Computer Methods in Applied Mechanics and Engineering 138(1–4):273–298
88. Électricité de France (2014) Code_aster. URL http://www.code-aster.org